PHYSICAL REVIEW D **88,** 054032 (2013)

Effective multiquark interactions with explicit breaking of chiral symmetry

A. A. Osipov,* B. Hiller,† and A. H. Blin‡

Departamento de Física da Universidade de Coimbra, Centro de Física Computacional, 3004-516 Coimbra, Portugal

(Received 3 October 2012; revised manuscript received 9 September 2013; published 30 September 2013)

In a long distance Lagrangian approach to the low lying meson phenomenology, we present and discuss the most general spin zero multiquark interaction vertices of nonderivative type which include a set of effective interactions proportional to the current quark masses, breaking explicitly the chiral $SU(3)_L \times SU(3)_R$ and $U_A(1)$ symmetries. These vertices are of the same order in N_c, counting as the 't Hooft flavor determinant interaction and the eight quark interactions which extend the original four quark interaction Lagrangian, leading in N_c, of Nambu and Jona-Lasinio. The N_c assignments match the counting rules based on arguments set by the scale of spontaneous chiral symmetry breaking. With path-integral bosonization techniques which appropriately take into account the quark mass differences, we derive the mesonic Lagrangian up to three-point mesonic vertices. We demonstrate that explicit symmetry breaking effects in interactions are essential to obtain the correct empirical ordering and magnitude of the splitting of certain states such as $m_K < m_\eta$ for the pseudoscalars and $m_{\kappa_0} < m_{a_0} \sim m_{f_0}$ in the scalar sector, and to achieve total agreement with the empirical low lying meson mass spectra. With all parameters of the model fixed by the spectra, we analyze further a bulk of two-body decays at the tree level of the bosonic Lagrangian: the strong decays of the scalars $\sigma \to \pi\pi$, $f_0(980) \to \pi\pi$, $\kappa(800) \to \pi K$, and $a_0(980) \to \pi\eta$, as well as the two photon decays of $a_0(980)$, $f_0(980)$, and σ mesons, and the anomalous decays of the pseudoscalars $\pi \to \gamma\gamma$, $\eta \to \gamma\gamma$, and $\eta' \to \gamma\gamma$. Our results for the strong decays are within the current expectations and the pseudoscalar radiative decays are in very good agreement with data. The radiative decays of the scalars are smaller than the observed values for the $f_0(980)$ and the σ, but reasonable for the a_0. A detailed discussion accompanies all the results.

DOI: 10.1103/PhysRevD.88.054032 PACS numbers: 12.39.Fe, 11.30.Qc, 11.30.Rd, 12.40.Yx

I. INTRODUCTION

A long history of applying the Nambu–Jona-Lasinio (NJL) model in hadron physics shows the importance of the concept of effective multiquark interactions for modeling QCD at low energies. Originally formulated in terms of the γ_5 gauge invariant nonlinear four-fermion coupling [1,2], the model has been extended to the realistic three flavor and color case with $U(1)_A$ breaking six-quark 't Hooft interactions [3–17] and an appropriate set of eight-quark interactions [18]. The last ones complete the number of vertices which are important in four dimensions for dynamical $SU(3)_L \times SU(3)_R$ chiral symmetry breaking [19,20].

The explicit breaking of chiral symmetry in the NJL model is described by introducing the standard light quark mass term of the QCD Lagrangian (light means consisting of u, d, and s quarks), e.g., [21,22]. The current quark mass dependence is of importance for several reasons, in particular for the phenomenological description of meson spectra and meson-meson interactions, and for the critical point search in hot and dense hadronic matter, where it has a strong impact on the phase diagram [23]. The values of the current quark masses are determined in the Higgs sector of the standard model. In this regard they are foreign to QCD and, at an effective description, can be included through the external sources, interacting with the originally massless quark fields. This is why the explicit chiral symmetry breaking (ChSB) by the standard mass term of the free Lagrangian is only a part of the more complicated picture arising in effective models beyond leading order [24]. Chiral perturbation theory [25–28] gives a well-known example of a self-consistent accounting of the mass terms, order by order, in an expansion in the masses themselves. In fact, extended NJL-type models should not be an exception from this rule. If one considers multiquark effective vertices, to the extent that $1/N_c$ suppressed 't Hooft and eight-quark terms are included in the Lagrangian, certain mass dependent multiquark interactions must be also taken into account.

The aim of the present work is precisely to analyze these higher order terms in the quark mass expansion. Our consideration proceeds along the following steps. We start from the three-flavor NJL-type model with self-interacting massless quarks. The $SU(3)_L \times SU(3)_R$ chiral symmetry of the Lagrangian is known to be dynamically broken to its $SU(3)_V$ subgroup at some scale Λ, with Λ being one of the model parameters. There is also explicit symmetry breaking due to the bare quark masses χ, which are taken to transform as $\chi = (3, 3^*)$ under $SU(3)_L \times SU(3)_R$. Since the Lagrangian contains, in general, an unlimited number of nonrenormalizable multiquark and χ-quark interactions

*osipov@nu.jinr.ru
†brigitte@teor.fis.uc.pt
‡alex@teor.fis.uc.pt

(scaled by some powers of Λ), we formulate the power counting rules to classify these vertices in accordance with their importance for dynamical symmetry breaking. Then we bosonize the theory by using the path-integral method. The functional integrals are calculated in the stationary phase approximation and by using the heat kernel technique. As a result one obtains the low-energy meson Lagrangian. At last we fix the parameters of the model by confronting it with the experimental data. In particular, we show the ability of the model to describe the spectrum of the pseudo-Goldstone bosons, including the fine-tuning of the η-η' splitting, and the spectrum of the light scalar mesons: σ or $f_0(500)$, $\kappa(800)$, $f_0(980)$, and $a_0(980)$.

The coupling constants of multiquark vertices, fixed from mass spectra, enter the expressions for meson decay amplitudes and lead to a bulk of model predictions. It is interesting to note that certain multiquark vertices of the model encode implicitly in the couplings of the tree level bosonized Lagrangian the signature of $q\bar{q}$ and more complex quark structures which are elsewhere obtained by considering explicitly meson loop corrections, tetraquark configurations, and so on [29–41]. It seems appropriate, therefore, to examine the possible physics opportunities connected with the discovery and study of such multiquark structures in hadrons. For instance, by calculating the mass spectra and the strong decays of the scalars, one can realize which multiquark interactions are most relevant at the scale of spontaneous ChSB. On the other hand, by analyzing the two photon radiative decays, where a different scale, associated with the electromagnetic interaction, comes into play, one can study the possible recombinations of quarks inside the hadron. We will show, for example, that the $a_0(980)$ meson couples with a large strength of the multiquark components to the two kaon channel in its strong decay to two pions, but evidences a dominant $q\bar{q}$ component in its radiative decay. As opposed to this, the σ and $f_0(980)$ mesons do not display an enhanced $q\bar{q}$ component either in their two photon decays or in the strong decays.

There are several direct motivations for this work. In the first place, the quark masses are the only parameters of the QCD Lagrangian which are responsible for the explicit ChSB, and it is important for the effective theory to trace this dependence in full detail. In this paper it will be argued that it is from the point of view of the $1/N_c$ expansion that the new quark mass dependent interactions must be included in the NJL-type Lagrangian already when the $U(1)_A$ breaking 't Hooft determinantal interaction is considered. This important point is somehow completely ignored in the current literature.

A second reason is that nowadays it is getting clear that the eight-quark interactions, which are almost inessential for the mesonic spectra in the vacuum, can be important for the quark matter in a strong magnetic background [42–46]. The simplest next possibility is to add to that picture a set of new effective quark mass–dependent interactions, discussed in this work. Such a feature of the quark matter has not been studied yet, but probably contains interesting physics.

Further motivation comes from the hadronic matter studies in a hot and dense environment. It is known that lattice QCD at finite density suffers from the numerical sign problem. This is why the phase diagram is notoriously difficult to compute *ab initio*, except for the extremely high density regime where perturbative QCD methods are applicable. In such circumstances, effective models designed to shed light on the phase structure of QCD are valuable, especially if such models are known to be successful in the description of the hadronic matter at zero temperature and density. Reasonable modifications of the NJL model are of special interest in this context and our work aims also at future applications in that area.

The paper is organized as follows. In Sec. II, the effective Lagrangian in terms of quark degrees of freedom and bosonic sources with specific quantum numbers is derived using a classification scheme which selects all possible nonderivative vertices according to the symmetries of the strong interaction and which are relevant at the scale Λ of spontaneous chiral symmetry breaking. It is then shown that this scheme can be equally organized in terms of the large N_c counting rules, which in turn allow us to attribute to the couplings of the interactions encoded signatures of $q\bar{q}$ and more complex structures involving four fermions. We obtain in this section also that a set of interactions leads to the Lagrangian specific Kaplan-Manohar ambiguity associated with the current quark masses.

In Sec. III we proceed to bosonize the multiquark Lagrangian in two steps. First, we introduce in Sec. III A a set of auxiliary scalar fields. By these new variables the multiquark interactions can be brought to the Yukawa form that is quadratic in Fermi fields. Consequently one obtains a Gauss-type integral over quarks and a set of integrals over auxiliary fields. The latter are evaluated by the stationary phase method. We obtain here the vertices up to the cubic power in the meson fields, needed for the study of the meson spectra and of the two-body decays. Then, in section III B, we integrate over quark fields. The arising quark determinant of the Dirac operator is a complicated nonlocal functional of the collective meson fields. We calculate it in the low-energy regime by using the Schwinger-DeWitt technique, based on the heat kernel expansion. In this approximation one can adequately incorporate the effect of different quark masses contained in the modulus of the one-loop quark determinant. We derive the kinetic terms of the collective meson fields, as well as the heat kernel part of contributions to meson masses and interactions. In the end of this section we present the complete bosonized Lagrangian, give the mixing angle conventions used, and the expressions for the strong decay widths. In Sec. III C

we obtain the expressions for the radiative widths of the pseudoscalars and scalars.

In Sec. IV we present the numerical results and discussion, in IV A for the meson mass spectra and weak decay constants, in IV B for the strong decays, and in IV C for the radiative decays.

We conclude in Sec. V with a summary of the main results.

II. EFFECTIVE MULTIQUARK INTERACTIONS

The chiral quark Lagrangian has predictive power for the energy range which is of order $\Lambda \simeq 4\pi f_\pi \sim 1$ GeV [47]. Λ characterizes the spontaneous chiral symmetry breaking scale. Consequently, the effective multiquark interactions, responsible for this dynamical effect, are suppressed by Λ, which provides a natural expansion parameter in the chiral effective Lagrangian. The scale above which these interactions disappear and QCD becomes perturbative enters the NJL model as an ultraviolet cutoff for the quark loops. Thus, to build the NJL-type Lagrangian we have only three elements: the quark fields q, the scale Λ, and the external sources χ, which generate explicit symmetry breaking effects—resulting in mass terms and mass-dependent interactions.

The color quark fields possess definite transformation properties with respect to the chiral flavor $U(3)_L \times U(3)_R$ global symmetry of the QCD Lagrangian with three massless quarks (in the large N_c limit). It is convenient to introduce the $U(3)$ Lie-algebra valued field $\Sigma = \frac{1}{2}(s_a - ip_a)\lambda_a$, where $s_a = \bar{q}\lambda_a q$, $p_a = \bar{q}\lambda_a i\gamma_5 q$, and $a = 0, 1, \ldots, 8$, and $\lambda_0 = \sqrt{2/3} \times 1$, λ_a being the standard $SU(3)$ Gell-Mann matrices for $1 \le a \le 8$. Under chiral transformations, $q' = V_R q_R + V_L q_L$, where $q_R = P_R q$, $q_L = P_L q$, and $P_{R,L} = \frac{1}{2}(1 \pm \gamma_5)$. Hence, $\Sigma' = V_R \Sigma V_L^\dagger$ and $\Sigma^{\dagger\prime} = V_L \Sigma^\dagger V_R^\dagger$. The transformation property of the source is supposed to be $\chi' = V_R \chi V_L^\dagger$.

Any term of the effective multiquark Lagrangian without derivatives can be written as a certain combination of fields which is invariant under chiral $SU(3)_R \times SU(3)_L$ transformations and conserves C, P, and T discrete symmetries. These terms have the general form

$$L_i \sim \frac{\bar{g}_i}{\Lambda^\gamma} \chi^\alpha \Sigma^\beta, \tag{1}$$

where $\bar{g}_i$ are dimensionless coupling constants [starting from Eq. (21) the dimensional couplings $g_i = \bar{g}_i/\Lambda^\gamma$ will also be considered]. Using dimensional arguments we find (in four dimensions) $\alpha + 3\beta - \gamma = 4$, with integer values for α, β, and γ.

We obtain a second restriction by considering only the vertices which make essential contributions to the gap equations in the regime of dynamical chiral symmetry breaking; i.e., we collect only the terms whose contributions to the effective potential survive at $\Lambda \to \infty$. We get this information by contracting quark lines in L_i and finding that this term contributes to the power counting of Λ in the effective potential as $\sim\Lambda^{2\beta-\gamma}$; i.e., we obtain that $2\beta - \gamma \ge 0$ (we used the fact that in four dimensions each quark loop contributes as Λ^2).

Combining both restrictions we come to the conclusion that only vertices with

$$\alpha + \beta \le 4 \tag{2}$$

must be taken into account in the approximation considered. On the basis of this inequality, one can conclude that (i) there are only four classes of vertices which contribute at $\alpha = 0$; those are four-, six-, and eight-quark interactions, corresponding to $\beta = 2$, 3, and 4, respectively (the $\beta = 1$ class is forbidden by chiral symmetry requirements); and (ii) there are only six classes of vertices depending on external sources χ. They are $\alpha = 1$, $\beta = 1$, 2, 3; $\alpha = 2$, $\beta = 1$, 2; and $\alpha = 3$, $\beta = 1$.

Let us consider now the structure of multiquark vertices in detail [48]. The Lagrangian corresponding to the case (i) is well known:

$$L_{\rm int} = \frac{\bar{G}}{\Lambda^2}\,{\rm tr}(\Sigma^\dagger\Sigma) + \frac{\bar{\kappa}}{\Lambda^5}({\rm det}\,\Sigma + {\rm det}\,\Sigma^\dagger) + \frac{\bar{g}_1}{\Lambda^8}({\rm tr}\Sigma^\dagger\Sigma)^2 + \frac{\bar{g}_2}{\Lambda^8}\,{\rm tr}(\Sigma^\dagger\Sigma\Sigma^\dagger\Sigma). \tag{3}$$

It contains four dimensionful couplings G, κ, g_1, g_2.

The second group (ii) contains 11 terms:

$$L_\chi = \sum_{i=0}^{10} L_i, \tag{4}$$

where

$$\begin{aligned}
L_0 &= -{\rm tr}(\Sigma^\dagger\chi + \chi^\dagger\Sigma)\\
L_1 &= -\frac{\bar{\kappa}_1}{\Lambda} e_{ijk}e_{mnl}\Sigma_{im}\chi_{jn}\chi_{kl} + {\rm H.c.}\\
L_2 &= \frac{\bar{\kappa}_2}{\Lambda^3} e_{ijk}e_{mnl}\chi_{im}\Sigma_{jn}\Sigma_{kl} + {\rm H.c.}\\
L_3 &= \frac{\bar{g}_3}{\Lambda^6}\,{\rm tr}(\Sigma^\dagger\Sigma\Sigma^\dagger\chi) + {\rm H.c.}\\
L_4 &= \frac{\bar{g}_4}{\Lambda^6}\,{\rm tr}(\Sigma^\dagger\Sigma)\,{\rm tr}(\Sigma^\dagger\chi) + {\rm H.c.}\\
L_5 &= \frac{\bar{g}_5}{\Lambda^4}\,{\rm tr}(\Sigma^\dagger\chi\Sigma^\dagger\chi) + {\rm H.c.}\\
L_6 &= \frac{\bar{g}_6}{\Lambda^4}\,{\rm tr}(\Sigma\Sigma^\dagger\chi\chi^\dagger + \Sigma^\dagger\Sigma\chi^\dagger\chi)\\
L_7 &= \frac{\bar{g}_7}{\Lambda^4}({\rm tr}\Sigma^\dagger\chi + {\rm H.c.})^2\\
L_8 &= \frac{\bar{g}_8}{\Lambda^4}({\rm tr}\Sigma^\dagger\chi - {\rm H.c.})^2\\
L_9 &= -\frac{\bar{g}_9}{\Lambda^2}\,{\rm tr}(\Sigma^\dagger\chi\chi^\dagger\chi) + {\rm H.c.}\\
L_{10} &= -\frac{\bar{g}_{10}}{\Lambda^2}\,{\rm tr}(\chi^\dagger\chi){\rm tr}(\chi^\dagger\Sigma) + {\rm H.c.}
\end{aligned} \tag{5}$$

Each term in the Lagrangian L_6 is Hermitian by itself, but because of the parity symmetry of strong interactions, which transforms one of them into the other, they have a common coupling $\bar{g}_6$.

Some useful insight into the Lagrangian above can be obtained by considering it from the point of view of the $1/N_c$ expansion. Indeed, the number of color components of the quark field q^i is N_c. Hence, summing over color indices in Σ gives a factor of N_c; i.e., one counts $\Sigma \sim N_c$.

The cutoff Λ that gives the right dimensionality to the multiquark vertices scales as $\Lambda \sim N_c^0 = 1$, as a direct consequence of the gap equations [see Eq. (37) below], which imply $1 \sim N_c G \Lambda^2$; on the other hand, since the leading quark contribution to the vacuum energy is known to be of order N_c, the first term in (3) is estimated as N_c, and we conclude that $G \sim 1/N_c$.

Furthermore, the $U(1)_A$ anomaly contribution [the second term in (3)] is suppressed by one power of $1/N_c$; it yields $\kappa \sim 1/N_c^3$.

The last two terms in (3) have the same N_c counting as the 't Hooft term. They are of order 1. Indeed, Zweig's rule–violating effects are always of order $1/N_c$ with respect to the leading order contribution $\sim N_c$. This reasoning helps us to find $g_1 \sim 1/N_c^4$. The term with $g_2 \sim 1/N_c^4$ is also $1/N_c$ suppressed. It represents the next-to-leading-order contribution with one internal quark loop in N_c counting. Such vertex contains the admixture of the four-quark component $\bar{q}q\bar{q}q$ to the leading quark-antiquark structure at $N_c \to \infty$.

Next, all terms in Eq. (5), except L_0, are of order 1. The argument is just the same as before: this part of the Lagrangian is obtained by successive insertions of the χ field (χ counts as $\chi \sim 1$) in place of Σ fields in the already-known $1/N_c$ suppressed vertices. It means that κ_1, g_9, $g_{10} \sim 1/N_c$; κ_2, g_5, g_6, g_7, $g_8 \sim 1/N_c^2$; and g_3, $g_4 \sim 1/N_c^3$.

There are two important conclusions here. The first is that at leading order in $1/N_c$ only two terms contribute: the first term of Eq. (3) and the first term of Eq. (5). This corresponds exactly to the standard NJL model picture, where mesons are pure $\bar{q}q$ states with constituents which have a nonzero bare mass. At the next-to-leading order, we have 13 terms additionally. They trace the Zweig's rule–violating effects (κ, κ_1, κ_2, g_1, g_4, g_7, g_8, g_{10}) and an admixture of the four-quark component to the $\bar{q}q$ one (g_2, g_3, g_5, g_6, g_9). Only the phenomenology of the last three terms from Eq. (3) has been studied until now. We must still understand the role of the other ten terms to be consistent with the generic $1/N_c$ expansion of QCD.

The second conclusion is that the N_c counting justifies the classification of the vertices made above on the basis of the inequality (2). This is seen as follows: the equivalent inequality $\lceil(\alpha+\beta)/2\rceil \le 2$ is obtained by restricting the multiquark Lagrangian to terms that do not vanish at $N_c \to \infty$ [it follows from (1) that $\beta - \lceil\gamma/2\rceil \ge 0$ by noting that $\bar{g}_i \sim 1/N_c^{\lceil\gamma/2\rceil}$, where $\lceil\gamma/2\rceil$ is the nearest integer greater than or equal to $\gamma/2$].

The total Lagrangian is the sum

$$L = \bar{q} i\gamma^\mu \partial_\mu q + L_{\rm int} + L_\chi. \tag{6}$$

In this $SU(3)_L \times SU(3)_R$ symmetric chiral Lagrangian we neglect terms with derivatives in the multiquark interactions, as usually assumed in the NJL model. We follow this approximation, because the specific questions for which these terms might be important, e.g., the radial meson excitations, or the existence of some inhomogeneous phases, characterized by a spatially varying order parameter, are not the goal of this work.

Finally, having all the building blocks conform with the symmetry pattern of the model, one is now free to choose the external source χ. Putting $\chi = \mathcal{M}/2$, where

$$\mathcal{M} = \mathrm{diag}(\mu_u, \mu_d, \mu_s),$$

we obtain a consistent set of explicitly breaking chiral symmetry terms. This leads to the following mass dependent part of the NJL Lagrangian:

$$L_\chi \to L_\mu = -\bar{q} m q + \sum_{i=2}^{8} L_i', \tag{7}$$

where the current quark mass matrix m is equal to

$$m = \mathcal{M} + \frac{\bar{\kappa}_1}{\Lambda}(\det \mathcal{M})\mathcal{M}^{-1} + \frac{\bar{g}_9}{4\Lambda^2}\mathcal{M}^3 + \frac{\bar{g}_{10}}{4\Lambda^2}(\mathrm{tr}\mathcal{M}^2)\mathcal{M}, \tag{8}$$

and

$$\begin{aligned}
L_2' &= \frac{\bar{\kappa}_2}{2\Lambda^3} e_{ijk} e_{mnl} \mathcal{M}_{im} \Sigma_{jn} \Sigma_{kl} + \mathrm{H.c.} \\
L_3' &= \frac{\bar{g}_3}{2\Lambda^6} \mathrm{tr}(\Sigma^\dagger \Sigma \Sigma^\dagger \mathcal{M}) + \mathrm{H.c.} \\
L_4' &= \frac{\bar{g}_4}{2\Lambda^6} \mathrm{tr}(\Sigma^\dagger \Sigma)\mathrm{tr}(\Sigma^\dagger \mathcal{M}) + \mathrm{H.c.} \\
L_5' &= \frac{\bar{g}_5}{4\Lambda^4} \mathrm{tr}(\Sigma^\dagger \mathcal{M} \Sigma^\dagger \mathcal{M}) + \mathrm{H.c.} \\
L_6' &= \frac{\bar{g}_6}{4\Lambda^4} \mathrm{tr}[\mathcal{M}^2(\Sigma\Sigma^\dagger + \Sigma^\dagger\Sigma)] \\
L_7' &= \frac{\bar{g}_7}{4\Lambda^4} (\mathrm{tr}\Sigma^\dagger \mathcal{M} + \mathrm{H.c.})^2 \\
L_8' &= \frac{\bar{g}_8}{4\Lambda^4} (\mathrm{tr}\Sigma^\dagger \mathcal{M} - \mathrm{H.c.})^2.
\end{aligned} \tag{9}$$

Let us note that there is a definite freedom in the definition of the external source χ. In fact, the sources

$$\begin{aligned}
\chi^{(c_i)} = \chi &+ \frac{c_1}{\Lambda}(\det \chi^\dagger)\chi(\chi^\dagger\chi)^{-1} + \frac{c_2}{\Lambda^2}\chi\chi^\dagger\chi \\
&+ \frac{c_3}{\Lambda^2}\mathrm{tr}(\chi^\dagger\chi)\chi,
\end{aligned} \tag{10}$$

with three independent constants c_i, have the same symmetry transformation property as χ. Therefore, we could have used $\chi^{(c_i)}$ everywhere that we used χ. As a result, we would come to the same Lagrangian with the following redefinitions of couplings:

$$\bar{\kappa}_1 \to \bar{\kappa}_1' = \bar{\kappa}_1 + \frac{c_1}{2}, \quad \bar{g}_5 \to \bar{g}_5' = \bar{g}_5 - \bar{\kappa}_2 c_1,$$
$$\bar{g}_7 \to \bar{g}_7' = \bar{g}_7 + \frac{\bar{\kappa}_2}{2} c_1, \quad \bar{g}_8 \to \bar{g}_8' = \bar{g}_8 + \frac{\bar{\kappa}_2}{2} c_1,$$
$$\bar{g}_9 \to \bar{g}_9' = \bar{g}_9 + c_2 - 2\bar{\kappa}_1 c_1, \quad \bar{g}_{10} \to \bar{g}_{10}' = \bar{g}_{10} + c_3 + 2\bar{\kappa}_1 c_1. \tag{11}$$

Since c_i are arbitrary parameters, this corresponds to a continuous family of equivalent Lagrangians. This family reflects the known Kaplan-Manohar ambiguity [49–52] in the definition of the quark mass, which means that several different parameter sets (11) may be used to represent the data. In particular, without loss of generality we can use the reparametrization freedom to obtain the set with $\bar{\kappa}_1' = \bar{g}_9' = \bar{g}_{10}' = 0$.

The effective multiquark Lagrangian can be written now as

$$L = \bar{q}(i\gamma^\mu \partial_\mu - m)q + L_{\rm int} + \sum_{i=2}^{8} L_i'. \tag{12}$$

It contains 18 parameters: the scale Λ; three parameters which are responsible for explicit chiral symmetry breaking μ_u, μ_d, μ_s; and 14 interaction couplings $\bar{G}$, $\bar{\kappa}$, $\bar{\kappa}_1$, $\bar{\kappa}_2$, $\bar{g}_1, \ldots, \bar{g}_{10}$. Three of them, $\bar{\kappa}_1$, $\bar{g}_9$, $\bar{g}_{10}$, contribute to the current quark masses m. Seven more describe the strength of multiquark interactions with explicit symmetry breaking effects. These vertices contain new details of the quark dynamics which have not been studied yet in any NJL-type models. We shall now see how important they are.

III. BOSONIZATION: MESON MASSES AND DECAYS

A. Stationary phase contribution

The model can be solved by path-integral bosonization of the quark Lagrangian (12). Indeed, following [7] we may equivalently introduce auxiliary fields $s_a = \bar{q}\lambda_a q$, $p_a = \bar{q} i\gamma_5 \lambda_a q$, and physical scalar and pseudoscalar fields $\sigma = \sigma_a \lambda_a$, $\phi = \phi_a \lambda_a$. In these variables, the Lagrangian is a bilinear form in quark fields (once the replacement has been done the quarks can be integrated out, giving us the kinetic terms for the physical fields ϕ and σ)

$$L = \bar{q}(i\gamma^\mu \partial_\mu - \sigma - i\gamma_5 \phi)q + L_{\rm aux},$$
$$L_{\rm aux} = s_a \sigma_a + p_a \phi_a - s_a m_a + L_{\rm int}(s, p) + \sum_{i=2}^{8} L_i'(s, p, \mu). \tag{13}$$

It is clear that after the elimination of the fields σ, ϕ by means of their classical equations of motion, one can rewrite this Lagrangian in its original form (12). The term bilinear in the quark fields in (13) will be integrated out using the heat kernel technique in the next subsection. The remaining higher order quark interactions collected in $L_{\rm aux}$ will be integrated in the stationary phase approximation (SPA). In terms of auxiliary bosonic variables, one has

$$L_{\rm int}(s, p) = L_{4q} + L_{6q} + L_{8q}^{(1)} + L_{8q}^{(2)},$$
$$L_{4q}(s, p) = \frac{\bar{G}}{2\Lambda^2}(s_a^2 + p_a^2),$$
$$L_{6q}(s, p) = \frac{\bar{\kappa}}{4\Lambda^5} A_{abc} s_a (s_b s_c - 3 p_b p_c),$$
$$L_{8q}^{(1)}(s, p) = \frac{\bar{g}_1}{4\Lambda^8}(s_a^2 + p_a^2)^2,$$
$$L_{8q}^{(2)}(s, p) = \frac{\bar{g}_2}{8\Lambda^8}[d_{abe} d_{cde}(s_a s_b + p_a p_b)(s_c s_d + p_c p_d) + 4 f_{abe} f_{cde} s_a s_c p_b p_d], \tag{14}$$

and the quark mass–dependent part is as follows:

$$L_2' = \frac{3\bar{\kappa}_2}{2\Lambda^3} A_{abc} \mu_a (s_b s_c - p_b p_c),$$
$$L_3' = \frac{\bar{g}_3}{4\Lambda^6} \mu_a [d_{abe} d_{cde} s_b (s_c s_d + p_c p_d) - 2 f_{abe} f_{cde} p_b p_c s_d],$$
$$L_4' = \frac{\bar{g}_4}{2\Lambda^6} \mu_b s_b (s_a^2 + p_a^2),$$
$$L_5' = \frac{\bar{g}_5}{4\Lambda^4} \mu_b \mu_d (d_{abe} d_{cde} - f_{abe} f_{cde})(s_a s_c - p_a p_c),$$
$$L_6' = \frac{\bar{g}_6}{4\Lambda^4} \mu_a \mu_b d_{abe} d_{cde} (s_c s_d + p_c p_d),$$
$$L_7' = \frac{\bar{g}_7}{\Lambda^4}(\mu_a s_a)^2, \quad L_8' = -\frac{\bar{g}_8}{\Lambda^4}(\mu_a p_a)^2, \tag{15}$$

where

$$A_{abc} = \frac{1}{3!} e_{ijk} e_{mnl} (\lambda_a)_{im} (\lambda_b)_{jn} (\lambda_c)_{kl}, \tag{16}$$

and the $U(3)$ antisymmetric f_{abc} and symmetric d_{abc} constants are standard.

Our final goal is to clarify the phenomenological role of the mass-dependent terms described by the Lagrangian densities of Eq. (15). We can gain some understanding of this by considering the low-energy meson dynamics which follows from our Lagrangian. For that we must exclude quark degrees of freedom in (13), e.g., by integrating them out from the corresponding generating functional. The standard Gaussian path integral leads us to the fermion determinant, which we expand by using a heat kernel technique [53–56]. The remaining part of the Lagrangian, $L_{\rm aux}$, depends on auxiliary fields which do not have kinetic terms. The equations of motion of such a static system are the extremum conditions

$$\frac{\partial L}{\partial s_a} = 0, \qquad \frac{\partial L}{\partial p_a} = 0, \tag{17}$$

which must be fulfilled in the neighborhood of the uniform vacuum state of the theory. To take this into account, one should shift the scalar field $\sigma \to \sigma + M$. The new σ field has a vanishing vacuum expectation value $\langle\sigma\rangle = 0$, describing small amplitude fluctuations about the vacuum, with M being the mass of constituent quarks. We seek solutions of Eq. (17) in the form

$$\begin{aligned} s_a^{st} &= h_a + h_{ab}^{(1)}\sigma_b + h_{abc}^{(1)}\sigma_b\sigma_c + h_{abc}^{(2)}\phi_b\phi_c + \cdots \\ p_a^{st} &= h_{ab}^{(2)}\phi_b + h_{abc}^{(3)}\phi_b\sigma_c + \cdots \end{aligned} \tag{18}$$

Equations (17) determine all coefficients of this expansion giving rise to a system of cubic equations to obtain h_a and the full set of recurrence relations to find higher order coefficients in (18). We can gain some insight into the physical meaning of these parameters if we calculate the Lagrangian density $L_{\rm aux}$ on the stationary trajectory. In fact, using the recurrence relations, we are led to the result

$$\begin{aligned} L_{\rm aux} = {} & h_a\sigma_a + \frac{1}{2}h_{ab}^{(1)}\sigma_a\sigma_b + \frac{1}{2}h_{ab}^{(2)}\phi_a\phi_b \\ & + \frac{1}{3}\sigma_a[h_{abc}^{(1)}\sigma_b\sigma_c + (h_{abc}^{(2)} + h_{bca}^{(3)})\phi_b\phi_c] + \cdots \end{aligned} \tag{19}$$

Indicated are all the terms which are necessary to analyze the mass spectra and two particle decays. Here h_a define the quark condensates, the quantities $h_{ab}^{(1)}$, $h_{ab}^{(2)}$ contribute to the masses of scalar and pseudoscalar states, and higher order h's are the couplings that measure the strength of the meson-meson interactions. The transition from the Lagrangian $L_{\rm aux}(s, p)$ in (13) to its form $L_{\rm aux}(\sigma, \phi)$ in (19) can be viewed as a Legendre transformation.

We proceed now to explain the details of determining h. We address first the coefficients h_a, $h_{ab}^{(1)}$, and $h_{ab}^{(2)}$. In particular, Eq. (17) states that $h_a = 0$, if $a \neq 0, 3, 8$, while h_α ($\alpha = 0, 3, 8$), after the convenient redefinition to the flavor indices $i = u, d, s$

$$h_\alpha = e_{\alpha i}h_i, \qquad e_{\alpha i} = \frac{1}{2\sqrt{3}}\begin{pmatrix} \sqrt{2} & \sqrt{2} & \sqrt{2} \\ \sqrt{3} & -\sqrt{3} & 0 \\ 1 & 1 & -2 \end{pmatrix}, \tag{20}$$

satisfy the following system of cubic equations:

$$\begin{aligned} & \Delta_i + \frac{\kappa}{4}t_{ijk}h_jh_k + \frac{h_i}{2}(2G + g_1h^2 + g_4\mu h) + \frac{g_2}{2}h_i^3 \\ & + \frac{\mu_i}{4}[3g_3h_i^2 + g_4h^2 + 2(g_5 + g_6)\mu_ih_i + 4g_7\mu h] \\ & + \kappa_2t_{ijk}\mu_jh_k = 0. \end{aligned} \tag{21}$$

Here $\Delta_i = M_i - m_i$; t_{ijk} is a totally symmetric quantity, whose nonzero components are $t_{uds} = 1$; there is no summation over the open index i, but we sum over the dummy indices, e.g., $h^2 = h_u^2 + h_d^2 + h_s^2$, $\mu h = \mu_u h_u + \mu_d h_d + \mu_s h_s$.

In particular, Eq. (8) reads in this basis

$$m_i = \mu_i\left(1 + \frac{g_9}{4}\mu_i^2 + \frac{g_{10}}{4}\mu^2\right) + \frac{\kappa_1}{2}t_{ijk}\mu_j\mu_k. \tag{22}$$

For the set $g_9 = g_{10} = \kappa_1 = 0$ the current quark mass m_i coincides precisely with the explicit symmetry breaking parameter μ_i.

Note that the factor multiplying h_i in the third term of Eq. (21) is the same for each flavor. This quantity also appears in all meson mass expressions, and there is no further dependence on the couplings G, g_1, g_4 involved for meson states with $a = 1, 2, \ldots, 7$. Thus, there is a freedom of choice which allows us to vary these couplings, condensates, and quark masses μ_i, without altering this part of the meson mass spectrum.

To obtain the coefficients $h_{ab}^{(i)}$, ($i = 1, 2$), in the Lagrangian $L_{\rm aux}$ (19), it is sufficient to collect in the stationary phase equations (17) only the terms linear in the fields, as can be seen from the structure of the solutions (18). Moreover, for any coefficient multiplying a certain number n of fields in $L_{\rm aux}$, it is required to consider terms only up to order $n - 1$ in fields in the expansion (18). For instance, the inverse matrices to $h_{ab}^{(1)}$ and $h_{ab}^{(2)}$ are

$$\begin{aligned} -2(h_{ab}^{(1)})^{-1} = {} & (2G + g_1h^2 + g_4\mu h)\delta_{ab} + 4g_1h_ah_b + 3A_{abc}(\kappa h_c + 2\kappa_2\mu_c) + g_2h_rh_c(d_{abe}d_{cre} + 2d_{ace}d_{bre}) \\ & + g_3\mu_rh_c(d_{abe}d_{cre} + d_{ace}d_{bre} + d_{are}d_{bce}) + 2g_4(\mu_ah_b + \mu_bh_a) + g_5\mu_r\mu_c(d_{are}d_{bce} - f_{are}f_{bce}) \\ & + g_6\mu_r\mu_cd_{abe}d_{cre} + 4g_7\mu_a\mu_b, \end{aligned} \tag{23}$$

$$\begin{aligned} -2(h_{ab}^{(2)})^{-1} = {} & (2G + g_1h^2 + g_4\mu h)\delta_{ab} - 3A_{abc}(\kappa h_c + 2\kappa_2\mu_c) + g_2h_rh_c(d_{abe}d_{cre} + 2f_{are}f_{bce}) \\ & + g_3\mu_rh_c(d_{abe}d_{cre} + f_{are}f_{bce} + f_{ace}f_{bre}) - g_5\mu_r\mu_c(d_{are}d_{bce} - f_{are}f_{bce}) + g_6\mu_r\mu_cd_{abe}d_{cre} - 4g_8\mu_a\mu_b. \end{aligned} \tag{24}$$

These coefficients are totally defined in terms of h_a and the parameters of the model. Equations (23) and (24) can be easily converted into explicit formulas for $h_{ab}^{(i)}$, ($i = 1, 2$).

Finally, to obtain the $h^{(i)}_{abc}$, $(i = 1, 2, 3)$, of the interactions involving three fields in $L_{\rm aux}$, one equates the factors of $\sigma_a\sigma_b$, $\phi_a\phi_b$, $\phi_a\sigma_b$ in (17) independently to zero. After some algebra, this results in the following expressions:

$$\begin{aligned} h^{(1)}_{abc} = \Big[& \frac{3\kappa}{4} A_{\bar a \bar b \bar c} + g_1(h_{\bar a}\delta_{\bar b \bar c} + 2h_{\bar c}\delta_{\bar a \bar b}) \\ & + g_2 h_{\bar r}\Big(d_{\bar a \bar b \bar p} d_{\bar r \bar c \bar p} + \frac{1}{2} d_{\bar a \bar r \bar p} d_{\bar b \bar c \bar p}\Big) \\ & + \frac{g_3}{4} m_{\bar r}(2 d_{\bar a \bar c \bar p} d_{\bar b \bar r \bar p} + d_{\bar b \bar c \bar p} d_{\bar a \bar r \bar p} - f_{\bar b \bar c \bar p} f_{\bar a \bar r \bar p}) \\ & + \frac{g_4}{2}(m_{\bar a}\delta_{\bar b \bar c} + 2m_{\bar c}\delta_{\bar a \bar b})\Big] h^{(1)}_{a\bar a} h^{(1)}_{b\bar b} h^{(1)}_{c\bar c} \end{aligned} \tag{25}$$

$$\begin{aligned} h^{(2)}_{abc} = \Big[& -\frac{3\kappa}{4} A_{\bar a \bar b \bar c} + g_1 h_{\bar a}\delta_{\bar b \bar c} \\ & + g_2 h_{\bar r}\Big(f_{\bar a \bar b \bar p} f_{\bar c \bar r \bar p} + \frac{1}{2} d_{\bar a \bar r \bar p} d_{\bar b \bar c \bar p}\Big) \\ & - \frac{g_3}{4} m_{\bar r}(2 f_{\bar a \bar c \bar p} f_{\bar b \bar r \bar p} + f_{\bar b \bar c \bar p} f_{\bar a \bar r \bar p} - d_{\bar b \bar c \bar p} d_{\bar a \bar r \bar p}) \\ & + \frac{g_4}{2} m_{\bar a}\delta_{\bar b \bar c}\Big] h^{(1)}_{a\bar a} h^{(2)}_{b\bar b} h^{(2)}_{c\bar c} \end{aligned} \tag{26}$$

$$\begin{aligned} h^{(3)}_{abc} = \Big[& -\frac{3\kappa}{2} A_{\bar a \bar b \bar c} + 2g_1 h_{\bar c}\delta_{\bar b \bar a} \\ & + g_2 h_{\bar r}(d_{\bar a \bar b \bar p} d_{\bar c \bar r \bar p} + f_{\bar r \bar a \bar p} f_{\bar c \bar b \bar p} + f_{\bar r \bar b \bar p} f_{\bar c \bar a \bar p}) \\ & + \frac{g_3}{2} m_{\bar r}(d_{\bar a \bar b \bar p} d_{\bar c \bar r \bar p} + f_{\bar b \bar c \bar p} f_{\bar a \bar r \bar p} + f_{\bar a \bar c \bar p} f_{\bar b \bar r \bar p}) \\ & + g_4 m_{\bar c}\delta_{\bar b \bar a}\Big] h^{(2)}_{a\bar a} h^{(2)}_{b\bar b} h^{(1)}_{c\bar c}. \end{aligned} \tag{27}$$

Contracting with $\phi_b\phi_c$ in Eq. (19), one sees that the term going with $h^{(2)}_{abc}$ is simply half the one going with $h^{(3)}_{bca}$, and $L_{\rm aux}$ simplifies to

$$\begin{aligned} L_{\rm aux} = & h_a\sigma_a + \frac{1}{2} h^{(1)}_{ab}\sigma_a\sigma_b + \frac{1}{2} h^{(2)}_{ab}\phi_a\phi_b \\ & + \sigma_a\Big(\frac{1}{3} h^{(1)}_{abc}\sigma_b\sigma_c + h^{(2)}_{abc}\phi_b\phi_c\Big) + \cdots \end{aligned} \tag{28}$$

Although there are five parameters κ, g_1, g_2, g_3, g_4 which appear explicitly in $h^{(i)}_{abc}$, they do not represent new freedom to fit the meson interaction dynamics, since they occur also in the $h^{(i)}_{ab}$; through the latter, the $h^{(i)}_{abc}$ depend implicitly also on six further parameters G, κ_2, g_5, g_6, g_7, g_8. All will be fixed by fitting the mass spectra and weak decay constants; see (38) and Sec. IV below.

B. The heat kernel contribution

We now turn our attention to the total Lagrangian of the bosonized theory. To write down this Lagrangian we should add the terms coming from integrating out the quark degrees of freedom in (13) to our result (28). Fortunately, the technicalities are known. We use the modified heat kernel technique [54–56] developed for the case of explicit chiral symmetry breaking. In the isospin limit, one can find all necessary details of such calculations, for instance, in [53]. For future reference, we apply it here to obtain the result for the more general case in which the strong isospin symmetry is broken.

From the vacuum to vacuum persistence amplitude in the spontaneous broken phase

$$\begin{aligned} & Z[\sigma, \phi] = \int \mathcal{D}q\mathcal{D}\bar q \exp\Big(i\int d^4x \mathcal{L}_q(\sigma, \phi)\Big), \\ & \mathcal{L}_q(\sigma, \phi) = \bar q(i\gamma^\mu\partial_\mu - M - \sigma - i\gamma_5\phi)q, \end{aligned} \tag{29}$$

the heat kernel result for the integration over the quark degrees of freedom is

$$\begin{aligned} & W[Y] = \ln|\det D| = -\frac{1}{2}\int_0^\infty \frac{dt}{t}\rho(t)\exp(-tD_E^\dagger D_E), \\ & D_E^\dagger D_E = M^2 - \partial^2 + Y, \\ & \quad Y = i\gamma_\mu(\partial_\mu + i\gamma_5\partial_\mu\phi) + \sigma^2 + \{M, \sigma\} + \phi^2 \\ & \qquad + i\gamma_5[\sigma + M, \phi], \end{aligned} \tag{30}$$

or

$$W[Y] = -\int \frac{d^4x_E}{32\pi^2}\sum_{i=0}^\infty I_{i-1}\,{\rm tr}[b_i], \tag{31}$$

where D_E stands for the Dirac operator in Euclidean space. We consider the expansion up to the third Seeley-DeWitt coefficient b_i

$$\begin{aligned} & b_0 = 1, \qquad b_1 = -Y, \\ & b_2 = \frac{Y^2}{2} + \frac{\lambda_3}{2}\Delta_{ud}Y + \frac{\lambda_8}{2\sqrt{3}}(\Delta_{us} + \Delta_{ds})Y, \end{aligned} \tag{32}$$

with $\Delta_{ij} = M_i^2 - M_j^2$. This order of the expansion takes into account the dominant contributions of the quark one-loop integrals I_i $(i = 0, 1, \ldots)$; these are the arithmetic average values $I_i = \frac{1}{3}[J_i(M_u^2) + J_i(M_d^2) + J_i(M_s^2)]$ where

$$J_i(m^2) = \int_0^\infty \frac{{\rm d}t}{t^{2-i}}\rho(t\Lambda^2)e^{-tm^2}, \tag{33}$$

with the Pauli-Villars regularization kernel [57,58]

$$\rho(t\Lambda^2) = 1 - (1 + t\Lambda^2)\exp(-t\Lambda^2). \tag{34}$$

In the following, we need therefore only to know two of them (the lowest order $\sim b_0$ contributes to the effective potential and is not needed in the present study)

$$J_0(m^2) = \Lambda^2 - m^2\ln\Big(1 + \frac{\Lambda^2}{m^2}\Big), \tag{35}$$

and

$$J_1(m^2) = \ln\Big(1 + \frac{\Lambda^2}{m^2}\Big) - \frac{\Lambda^2}{\Lambda^2 + m^2}. \tag{36}$$

While both terms proportional to b_1 and b_2 have contributions to the gap equations and meson masses, only b_2 contributes to the kinetic and interaction terms. The σ tadpole term must be excluded from the total Lagrangian. This gives us a system of gap equations

$$h_i + \frac{N_c}{6\pi^2} M_i [3I_0 - (3M_i^2 - M^2) I_1] = 0. \tag{37}$$

Here $N_c = 3$ is the number of colors, and $M^2 = M_u^2 + M_d^2 + M_s^2$. Combining all terms of the total Lagrangian $L = L_{\rm kin} + L_{\rm mass} + L_{\rm int}$ that contribute to the kinetic terms $L_{\rm kin}$ and meson masses $L_{\rm mass}$, one gets

$$\begin{aligned} L_{\rm kin} + L_{\rm mass} = {} & \frac{N_c I_1}{16\pi^2} \,{\rm tr}[(\partial_\mu \sigma)^2 + (\partial_\mu \phi)^2] + \frac{N_c I_0}{4\pi^2}(\sigma_a^2 + \phi_a^2) - \frac{N_c I_1}{12\pi^2}\{[2(M_u + M_d)^2 - M_u M_d - M_s^2](\sigma_1^2 + \sigma_2^2) \\ & + [2(M_u + M_s)^2 - M_u M_s - M_d^2](\sigma_4^2 + \sigma_5^2) + [2(M_d + M_s)^2 - M_d M_s - M_u^2](\sigma_6^2 + \sigma_7^2) \\ & + \frac{1}{2}[\sigma_u^2(8M_u^2 - M_d^2 - M_s^2) + \sigma_d^2(8M_d^2 - M_u^2 - M_s^2) + \sigma_s^2(8M_s^2 - M_u^2 - M_d^2)] \\ & + \frac{1}{2}[\phi_u^2(2M_u^2 - M_d^2 - M_s^2) + \phi_d^2(2M_d^2 - M_u^2 - M_s^2) + \phi_s^2(2M_s^2 - M_u^2 - M_d^2)] \\ & + [2(M_u - M_d)^2 + M_u M_d - M_s^2](\phi_1^2 + \phi_2^2) + [2(M_u - M_s)^2 + M_u M_s - M_d^2](\phi_4^2 + \phi_5^2) \\ & + [2(M_d - M_s)^2 + M_d M_s - M_u^2](\phi_6^2 + \phi_7^2)\} + \frac{1}{2} h_{ab}^{(1)} \sigma_a \sigma_b + \frac{1}{2} h_{ab}^{(2)} \phi_a \phi_b. \end{aligned} \tag{38}$$

The kinetic term requires a redefinition of meson fields,

$$\sigma_a = g\sigma_a^R, \qquad \phi_a = g\phi_a^R, \qquad g^2 = \frac{4\pi^2}{N_c I_1}, \tag{39}$$

to obtain the standard factor $1/4$. The flavor and charged fields are related through

$$\begin{aligned} \frac{\lambda_a}{\sqrt{2}}\phi_a &= \begin{pmatrix} \frac{\phi_u}{\sqrt{2}} & \pi^+ & K^+ \\ \pi^- & \frac{\phi_d}{\sqrt{2}} & K^0 \\ K^- & \bar{K}^0 & \frac{\phi_s}{\sqrt{2}} \end{pmatrix} \\ \frac{\lambda_a}{\sqrt{2}}\sigma_a &= \begin{pmatrix} \frac{\sigma_u}{\sqrt{2}} & a_0^+ & \kappa^+ \\ a_0^- & \frac{\sigma_d}{\sqrt{2}} & \kappa^0 \\ \kappa^- & \bar{\kappa}^0 & \frac{\sigma_s}{\sqrt{2}} \end{pmatrix} \end{aligned} \tag{40}$$

and in particular for the diagonal components,

$$\begin{aligned} \phi_u &= \phi_3 + \frac{\sqrt{2}\phi_0 + \phi_8}{\sqrt{3}} = \phi_3 + \eta_{ns} \\ \phi_d &= -\phi_3 + \frac{\sqrt{2}\phi_0 + \phi_8}{\sqrt{3}} = -\phi_3 + \eta_{ns} \\ \phi_s &= \sqrt{\frac{2}{3}}\phi_0 - \frac{2\phi_8}{\sqrt{3}} = \sqrt{2}\eta_s, \end{aligned} \tag{41}$$

and similar for the scalar fields. Here we also introduce the η_{ns} and η_s which stand for the flavor components of the physical η, η' states in the nonstrange and strange basis. In addition to the flavor mixing in the η, η' channels, the isospin breaking induces a coupling between the π^0 and these states

$$\pi^0 = \phi_3 + \epsilon\eta + \epsilon'\eta'. \tag{42}$$

To get the physical π^0, η, and η' mesons and correspondingly the scalar $a_0^0(980)$, σ, and $f_0(980)$ mesons, one may proceed as in [59]. Since ϕ_3 couples weakly to the η_{ns} and η_s states (decoupling in the isospin limit) while the η-η' mixing is strong, it is appropriate to use isoscalar η_{ns}, η_s and isovector ϕ_3 combinations as a starting point for a unitary transformation to the physical meson states π^0, η, η'. In this case, the corresponding unitary matrix $\mathcal{U}$ can be linearized in the π^0-η and π^0-η' mixing angles $\epsilon_1, \epsilon_2 \sim \mathcal{O}(\epsilon)$, $\epsilon \ll 1$. Precisely [59]

$$\begin{pmatrix} \pi^0 \\ \eta \\ \eta' \end{pmatrix} = \mathcal{U}(\epsilon_1, \epsilon_2, \psi) \begin{pmatrix} \phi_3 \\ \eta_{ns} \\ \eta_s \end{pmatrix}, \tag{43}$$

where

$$\mathcal{U} = \begin{pmatrix} 1 & \epsilon_1 + \epsilon_2 \cos\psi & -\epsilon_2 \sin\psi \\ -\epsilon_2 - \epsilon_1 \cos\psi & \cos\psi & -\sin\psi \\ -\epsilon_1 \sin\psi & \sin\psi & \cos\psi \end{pmatrix}. \tag{44}$$

In particular, in Eq. (42) $\epsilon = \epsilon_2 + \epsilon_1 \cos\psi$, $\epsilon' = \epsilon_1 \sin\psi$.

In the isospin limit, we use the mixing angle conventions summarized in Appendix B of [58]. We have the following different possibilities of relating the physical states $(\bar{X}, X)$ with the states of the strange-nonstrange basis:

$$\begin{pmatrix} \bar{X} \\ X \end{pmatrix} = R_\psi \begin{pmatrix} X_{ns} \\ X_s \end{pmatrix} = R_{\bar{\psi}} \begin{pmatrix} -X_s \\ X_{ns} \end{pmatrix}, \tag{45}$$

where the orthogonal 2×2 matrix R_ψ is

$$R_\psi = \begin{pmatrix} \cos\psi & -\sin\psi \\ \sin\psi & \cos\psi \end{pmatrix}, \tag{46}$$

or of the singlet-octet basis

$$\begin{pmatrix} \bar{X} \\ X \end{pmatrix} = R_\theta \begin{pmatrix} X_8 \\ X_0 \end{pmatrix}. \tag{47}$$

Here θ, being a solution of the equation $\tan 2\theta = x$, is the principal value of $\arctan x$; i.e., it belongs to the interval $-(\pi/4) \le \theta \le (\pi/4)$. The angle ψ is related with θ by the equation $\psi = \theta + \bar{\theta}_{id}$, where $\bar{\theta}_{id}$ ($\theta_{id} + \bar{\theta}_{id} = \pi/2$) is determined by the equations $\sin\bar{\theta}_{id} = \sqrt{2/3}$, $\cos\bar{\theta}_{id} = 1/\sqrt{3}$; therefore, $\psi = \theta + \arctan\sqrt{2} = \theta + 54.74°$. It means that ψ is restricted to the range $9.74° \le \psi \le 99.74°$. If the value of ψ leaves the range, we must resort to the angle $\bar{\psi} = \psi - (\pi/2) = \theta - \theta_{id}$, taking values in the interval $-80.26° \le \bar{\psi} \le 9.74°$. These two angles correspond to two alternative phase conventions for a strange $\bar{s}s$ component. As a result of the following numerical calculations, in the case of the pseudoscalars the identification of the physical states is $\bar{X} = \eta$, $X = \eta'$ and for the scalars $\bar{X} = f_0(980)$, $X = \sigma$.

We turn to the interaction terms of the heat kernel action in (30). The only contribution comes from $Y^2/2$ in the term proportional to b_2 and reads

$$L_{\rm int}^{(hk)} = -\frac{N_c}{2\pi^2} I_1 M_a [d_{ab\rho} d_{ce\rho} \sigma_b (\sigma_c \sigma_e + \phi_c \phi_e) + 2 f_{ac\rho} f_{be\rho} \sigma_b \phi_c \phi_e], \tag{48}$$

which must be added to the interaction piece stemming from (28), yielding the total interaction Lagrangian

$$L_{\rm int} = L_{\rm int}^{(hk)} + \sigma_a \left(\frac{1}{3} h^{(1)}_{abc} \sigma_b \sigma_c + h^{(2)}_{abc} \phi_b \phi_c \right). \tag{49}$$

Note that all dependence on the parameters of the explicit symmetry breaking quark interactions is explicitly absorbed in the bosonized Lagrangian through the matrices $h^{(1,2)}_{ab}$ for the meson mass spectra (38) and through the $h^{(1,2,3)}_{abc}$ for the meson interaction Lagrangian (49). In other words, the formal structure of the Lagrangian (28) in comparison to the case without these interactions remains unchanged. This differs from the heat kernel Lagrangian where the information about the difference in constituent quark masses leads to a resummation of the heat kernel series for the modified Seeley-DeWitt coefficients b_i [54–56]. The parameters of these two seemingly separated sectors of the Lagrangian, i.e., the constituent quark masses and scale parameter Λ for the heat kernel Lagrangian on one hand, and the multiquark interaction couplings for the SPA piece on the other hand, are connected through the gap equations (37) which must be solved self-consistently with the SPA equations (21).

In the remainder of this subsection, we discuss the scheme in which the strong decay widths of the scalar mesons are calculated. Given the complexity of the Lagrangian, we will restrict our study of the decays to the tree level bosonic couplings (48) and (49). To deal in an approximate way with the proximity of particle thresholds to the resonance mass, we shall resort to the widely accepted Flatté-type distribution [60]. Other closed bosonic channel contributions will not be taken into consideration for simplicity, since the ratios of couplings in the concurring closed channels to the nominal one turn out to be numerically less relevant in our fits.

The strong decay width of the scalar meson S in two pseudoscalars P_1, P_2 are thus obtained as

$$\Gamma_\beta = \frac{|\vec{p}_\beta|}{8\pi m_S^2} |g_\beta|^2 \equiv \bar{g}_\beta |\vec{p}_\beta| \tag{50}$$

with

$$|\vec{p}_\beta| = \sqrt{\frac{[m_S^2 - (m_1 + m_2)^2][m_S^2 - (m_1 - m_2)^2]}{4m_S^2}},$$

where index β specifies all necessary kinematic characteristics of the channel $S \to P_1 P_2$, and the masses m_S, m_1, m_2 of the states. We introduce also a shorthand notation for the dimensionless quantity $\bar{g}_\beta$ in Eq. (50). In this definition we include all flavor and symmetry factors associated with the final state.

The widths so obtained are valid in the Breit-Wigner resonance scheme, which is known to be an incomplete description for decays with the resonance mass close to the threshold of particle emission. We use Flatté distributions in the cases of the $a_0(980)$ and $f_0(980)$ decays to accommodate the threshold effects associated with the two kaon production, on grounds of analyticity and unitarity at the threshold. Close to this threshold, the elastic scattering cross section for $\pi\eta$ in the case of a_0 or $\pi\pi$ for f_0 is parametrized by a two-channel resonance

$$\sigma_{el} = 4\pi |f_{el}|^2, \qquad f^\beta_{el} = \frac{1}{|\vec{p}_\beta|} \frac{m_R \Gamma_\beta}{m_R^2 - s - i m_R (\Gamma_\beta + \Gamma^S_{K\bar{K}})}, \tag{51}$$

with the index β designating here either the $a_0\pi\eta$ or the $f_0\pi\pi$ channels and

$$\Gamma^S_{K\bar{K}} = \begin{cases} \bar{g}^S_K \sqrt{\frac{s}{4} - m_K^2} & \text{above threshold} \\ i\bar{g}^S_K \sqrt{m_K^2 - \frac{s}{4}} & \text{below threshold} \end{cases}, \tag{52}$$

where $\bar{g}^S_K$ stands for the coupling of S to the two kaons, in this case $S = a_0$ or f_0. Here m_R is the nominal resonance mass and $s = (p_1 + p_2)^2$, where p_1, p_2 are the 4-momenta of P_1 and P_2. Near the $K\bar{K}$ threshold only the width $\Gamma^S_{K\bar{K}}$ is expected to vary strongly; the widths Γ_β are approximated by a constant value in this region, taken to be (50) evaluated at $s = m_R^2$, since the $\pi\eta$ and $\pi\pi$ thresholds lie

further away from the resonance. The numerical results are presented and discussed in Sec. IV.

C. A note on radiative decays

Additional information on the structure of the mesons is obtained through the study of their radiative decays. We consider in this work the two photon decays at the quark one-loop order of the scalar and pseudoscalar mesons. The corresponding integrals are finite. A direct extension of the heat kernel Lagrangian to incorporate the coupling to the electromagnetic interaction shows that there is no contribution up to the order b_2 of the Seeley-DeWitt coefficients for the scalar decays. The anomalous pseudoscalar–two photon decays belong to the imaginary part of the action and are not contemplated by the heat kernel techniques considered, which apply only to the real part. By the Adler-Bardeen theorem [61–63] they are fully determined by the three-point function Feynman amplitudes involving one quark loop; higher orders only redefine the couplings. There is however a source of uncertainty which resides in the model-dependent determination of the coupling of the η and η' mesons to the quarks. In our approach they are calculated within the heat kernel technique outlined in Sec. III B. Regarding the scalar meson two photon decays, they are also most simply evaluated through the three-point Feynman amplitudes, keeping only the contribution corresponding to the first nonvanishing order in the heat kernel action, that is, the term involving the Seeley-DeWitt coefficient b_3. From now on we will consider the case with exact $SU(2)$ isospin symmetry, i.e., $\mu_u = \mu_d = \hat{\mu} \neq \mu_s$ and $M_u = M_d = \hat{M} \neq M_s$. With the standard electromagnetic coupling to quarks $\mathcal{L}_\gamma = -e\bar{q}\gamma^\mu Q q A_\mu$, $Q = \frac{1}{2}(\lambda_3 + \frac{1}{\sqrt{3}}\lambda_8)$ and using the Pauli-Villars regularization, the scalar meson to two photons amplitude A: $S(s) \to \gamma(p_1, \epsilon_\mu^*) + \gamma(p_2, \epsilon_\nu^*)$ is obtained in terms of the gauge invariant tensor $\mathcal{L}_{\mu\nu} = (p_2^\mu p_1^\nu - \frac{1}{2} s g^{\mu\nu})$, with $s = (p_1 + p_2)^2$

$$
\begin{aligned}
&A^{\mu\nu}_{S\gamma\gamma} = \mathcal{L}^{\mu\nu} A_{S\gamma\gamma}; \qquad S = \sigma, f_0(980), a_0(980)\\
&A_{\sigma\gamma\gamma} = \frac{5}{9} T_u \cos\bar{\psi} - \frac{\sqrt{2}}{9} T_s \sin\bar{\psi}\\
&A_{f_0\gamma\gamma} = -\frac{5}{9} T_u \sin\bar{\psi} - \frac{\sqrt{2}}{9} T_s \cos\bar{\psi} \qquad A_{a_0\gamma\gamma} = \frac{1}{3} T_u,
\end{aligned}
\tag{53}
$$

where

$$
\begin{aligned}
T_i &= 32\pi\alpha g M_i Q_3(s, M_i), \quad \mathrm{i} = (\mathrm{u}, \mathrm{s})\\
Q_3(s, M_i) &= \frac{iN_c}{16\pi^2} \int_0^1 dx \int_0^{1-x} dy (1 - 4xy)\\
&\quad \times \int_0^\infty dt \rho(t\Lambda^2) e^{-t(M_i^2 - xys).}
\end{aligned}
\tag{54}
$$

$\alpha = \frac{e^2}{4\pi}$ is the fine structure constant and g the field normalization defined in (39). The factors of T_i result from the flavor traces and projection to the physical states with the angle $\bar{\psi}$ defined in (45). The result for the integral $Q_3(s, M_i)$ with the Pauli-Villars kernel $\rho(t\Lambda^2)$ [Eq. (34)] has been evaluated in [64]. To obtain the dominant contribution, i.e., the first nonvanishing order in the heat kernel series, one needs to express the integrals $Q_3(s, M_i)$ as the following averaged sum evaluated at $s = 0$ [55,56]:

$$
\begin{aligned}
Q_3(0, M_i) \to Q_3(0, M_u, M_s) &= \frac{1}{3}(2Q_3(0, M_u) + Q_3(0, M_s))\\
&\quad + \mathcal{O}(b_3),
\end{aligned}
\tag{55}
$$

where the term $\mathcal{O}(b_3)$ is discarded as it belongs to the next order in the heat kernel series (30), and

$$
Q_3(0, M_i) = -\frac{N_c}{48\pi^2 M_i^2} \left(\frac{\Lambda^2}{\Lambda^2 + M_i^2}\right)^2, \tag{56}
$$

or, in the notation of (33), we have that

$$
Q_3(0, M_i) = -\frac{N_c}{48\pi^2} J_2(M_i^2). \tag{57}
$$

Finally the decay widths for the scalar mesons in the narrow width approximation are given as [see also (64)]

$$
\Gamma_{S\gamma\gamma} = \frac{m_S^3}{64\pi} |A_{S\gamma\gamma}|^2. \tag{58}
$$

The anomalous decay of the pseudoscalars $P = (\pi^0, \eta, \eta')$ in two photons $P(p) \to \gamma(p_1, \epsilon_\mu^*) + \gamma(p_2, \epsilon_\nu^*)$ has the same Lorentz structure in all channels and reads

$$
\begin{aligned}
A^{\mu\nu}_{P\gamma\gamma} &= \epsilon^{\mu\nu\alpha\beta} p_{1\alpha} p_{2\beta} A_{P\gamma\gamma}\\
A_{\eta\gamma\gamma} &= -\frac{5}{9} T_u^P \sin\bar{\psi}_P - \frac{\sqrt{2}}{9} T_s^P \cos\bar{\psi}_P\\
A_{\eta'\gamma\gamma} &= \frac{5}{9} T_u^P \cos\bar{\psi}_P - \frac{\sqrt{2}}{9} T_s^P \sin\bar{\psi}_P\\
A_{\pi^0\gamma\gamma} &= \frac{1}{3} T_u^P,
\end{aligned}
\tag{59}
$$

where $\bar{\psi}_P$ stands for the mixing angle in the pseudoscalar channels [Eq. (45)] and

$$
\begin{aligned}
T_i^P(s, M_i) &= 32\pi\alpha g M_i I_P(s, M_i)\\
I_P(s, M) &= \frac{-N_c}{16\pi^2} \int_0^1 dx \int_0^{1-x} dy \int_0^\infty dt e^{-t(M^2 - xys)},
\end{aligned}
\tag{60}
$$

and the contribution to the imaginary part of the heat kernel action is

$$
I_P(0, M) = \frac{-N_c}{32\pi^2 M^2}. \tag{61}
$$

At this stage one sees that the only parameter dependence in the radiative decays of the scalars and pseudoscalars

enters through the wave function normalization g, common to all decays considered, and through the constituent quark masses; there is also an explicit dependence on the scale Λ in the case of the scalar decays through the factor $(\frac{\Lambda^2}{\Lambda^2+M^2})^2$ in (56). The partial conservation of axial current hypothesis establishes a relation between g, the weak pion and kaon decay couplings, and the constituent quark masses [see also (66) below]

$$f_\pi = \frac{\hat{M}}{g}; \qquad f_K = \frac{\hat{M}+M_s}{2g}. \tag{62}$$

These identities allow us to eliminate all dependence on the constituent quark masses from the pseudoscalar radiative decays, leading to

$$T^P(0,\hat{M}) = \frac{N_c\alpha}{\pi f_\pi}, \qquad T^P(0,M_s) = \frac{N_c\alpha}{\pi(2f_K - f_\pi)}. \tag{63}$$

One then obtains the celebrated relation $A_{\pi\gamma\gamma} = \frac{\alpha}{\pi f_\pi}$ for the π^0 decay amplitude [61]. The Adler-Bardeen theorem allows us to infer that the study and measurement of the anomalous decays are a reliable means of determination of the mixing angle of the η and η' mesons, which must comply with the mixing angle determination extracted from the mass spectrum. One should also stress that with the present model Lagrangian one is able to account properly for the $SU(3)$ breaking effects in the description of the weak decay constants f_π and f_K, in addition to having the correct empirical η and η' meson masses (see Sec. IV), which has been an open problem until now. This is important for the numerical consistency in the amplitudes (63).

The respective widths are calculated as

$$\Gamma_{P\gamma\gamma} = \frac{|\vec{p}|^3}{8\pi}|A_{P\gamma\gamma}|^2, \tag{64}$$

with $|\vec{p}| = \sqrt{m_P^2/4}$ and m_P the pseudoscalar mass. The numerical results are presented in Sec. IV.

IV. FIXING PARAMETERS, NUMERICAL RESULTS AND DISCUSSION

A. Meson spectra and weak decays

In the chiral limit, $m_u = m_d = m_s = 0$, the Lagrangian (38) leads to the conserved vector, $\mathcal{V}^a_\mu$, and axial-vector, $\mathcal{A}^a_\mu$, currents. The matrix elements of axial-vector currents

$$\langle 0|\mathcal{A}^a_\mu(0)|\phi^b_R(p)\rangle = ip_\mu f^{ab} \tag{65}$$

define the weak and electromagnetic decay constants of physical pseudoscalar states (see details in [53]). Now let us fix the values of the various quantities introduced. After choosing the set $\kappa_1 = g_9 = g_{10} = 0$ we still have to fix 14 parameters: Λ, $\hat{m}$, m_s, G, κ, κ_2, and $g_1, \ldots, g_8$. There are two intrinsic restrictions of the model, namely, the stationary phase (21) and the gap (37) equations, which as mentioned above must be solved self-consistently. This is how the explicit symmetry breaking is intertwined with the dynamical symmetry breaking and vice versa. We use (37) to determine $\hat{h}$, h_s through Λ, M_s and $\hat{M}$. The ratio $M_s/\hat{M}$ is related to the ratio of the weak decay constants of the pion, $f_\pi = 92$ MeV, and the kaon, $f_K = 113$ MeV. Here we obtain

$$\frac{M_s}{\hat{M}} = 2\frac{f_K}{f_\pi} - 1 = 1.46. \tag{66}$$

Furthermore, the two Eqs. (21) can be used to find the values of Λ and $\hat{M}$ if the parameters $\hat{m}$, m_s, G, κ, κ_2, $g_1, \ldots, g_7$ are known. Thus, together with g_8 we have at this stage 13 couplings to be fixed. Let us consider the current quark masses $\hat{m}$ and m_s to be an input. Their values are known, from various analyses of the chiral treatment of the light pseudoscalars, to be around $\hat{m} = 4$ MeV and $m_s = 100$ MeV [65]. Then the remaining 11 couplings can be found by comparing with empirical data. One should stress the possibility (which did not exist before the inclusion of mass-dependent interactions) to fit the low lying pseudoscalar spectrum, $m_\pi = 138$ MeV, $m_K = 494$ MeV, $m_\eta = 547$ MeV, $m_{\eta'} = 958$ MeV, the weak pion and kaon decay constants, $f_\pi = 92$ MeV, $f_K = 113$ MeV, and the singlet-octet mixing angle $\theta_p = -15°$ to perfect accuracy; see Table I.

One can deduce that the couplings κ_2 and g_8 are essential to improve the description in the pseudoscalar sector; in particular, g_8 is responsible for fine-tuning the η-η' mass splitting (see also Table II), where the difference in g_8 between set (b) and sets (a), (c), (d) is due to the input $\theta_P = -15°$ versus $\theta_P = -12°$, respectively.

The remaining five conditions are taken from the scalar sector of the model. Unfortunately, the scalar channel in the region about 1 GeV became a long-standing problem of QCD. The abundance of meson resonances with 0^{++} quantum numbers shows that one can expect the presence of non-$q\bar{q}$ scalar objects, like glueballs, hybrids, multiquark states, and so forth [41]. This creates known difficulties in the interpretation and classification of scalars. For instance, the numerical attempts to organize the $U(3)$ quark-antiquark nonet based on the light scalar mesons, σ or $f_0(600)$, $a_0(980)$, $\kappa(800)$, $f_0(980)$, in the framework of

TABLE I. The same values for the pseudoscalar and scalar masses (except for m_σ) and weak decay constants (all in MeV) are used as input (marked with *) for different sets of the model. Parameter sets (a), (b), (c), (d) of all following tables differ by varying the mixing angles and m_σ: sets (a), (b), and (d) with $m_\sigma = 550$ MeV versus set (c) with $m_\sigma = 600$ MeV; sets (a), (c), and (d) with $\theta_P = -12°$ versus set (b) with $\theta_P = -15°$. The scalar mixing angle is kept constant, $\theta_S = 25°$, in (a), (b), (c) and increased to $\theta_S = 27.5°$ in set (d).

m_π	m_K	m_η	$m_{\eta'}$	f_π	f_K	m_κ	m_{a_0}	m_{f_0}
138*	494*	547*	958*	92*	113*	850*	980*	980*

TABLE II. Parameter sets of the model: $\hat{m}$, m_s, and Λ are given in MeV. The couplings have the following units: $[G] = \mathrm{GeV}^{-2}$, $[\kappa] = \mathrm{GeV}^{-5}$, $[g_1] = [g_2] = \mathrm{GeV}^{-8}$. We also show here the values of constituent quark masses $\hat{M}$ and M_s in MeV. See also the caption of Table I.

Sets	$\hat{m}$	m_s	$\hat{M}$	M_s	Λ	G	$-\kappa$	g_1	g_2
a	4.0*	100*	372	541	830	9.74	121.1	3136	133
b	4.0*	100*	372	542	829	9.83	118.5	3305	−158
c	4.0*	100*	370	539	830	10.45	120.3	2081	102
d	4.0*	100*	373	544	828	10.48	122.0	3284	173

NJL-type models, have failed (see, e.g., [8–10,58,66–68]). The reason is the ordering of the calculated spectrum which typically is $m_\sigma < m_{a_0} < m_\kappa < m_{f_0}$, as opposed to the empirical evidence: $m_\kappa < m_{a_0} \simeq m_{f_0}$.

On the other hand, it is known that a unitarized nonrelativistic meson model can successfully describe the light scalar meson nonet as $\bar{q}q$ states with a meson-meson admixture [33]. Another model which assumes the mixing of $q\bar{q}$ states with others, consisting of two quarks and two antiquarks, $q^2\bar{q}^2$ [29], yields a possible description of the 0^{++} meson spectra as well [38,39]. The well-known model of Close and Törnqvist [40] is also designed to describe two scalar nonets (above and below 1 GeV). The light scalar nonet below 1 GeV has a core made of $q^2\bar{q}^2$ states with a small admixture of a $\bar{q}q$ component, rearranged asymptotically as meson-meson states. These successful solutions seemingly indicate on the importance of certain admixtures for the correct description of the light scalars. Our model contains such admixtures in the form of the appropriate effective multiquark vertices with the asymptotic meson states described by the bosonized $\bar{q}q$ fields. We have found that the quark mass–dependent interactions can solve the problem of the light scalar spectrum and these masses can be understood in terms of spontaneous and explicit chiral symmetry breaking only. Indeed, one can easily fit the data: $m_\sigma = 600$ MeV, $m_{a_0} = 980$ MeV, $m_\kappa = 850$ MeV, $m_{f_0} = 980$ MeV. In this case we obtain for the singlet-octet mixing angle θ_s roughly $\theta_s = 19°$ [48]. Without changing the mass spectra, better fits for the strong radiative decays of the scalars are obtained with $\theta_s = 25° \div 28°$, in the next subsection.

We obtain and understand the empirical mass assignment inside the light scalar nonet as a consequence of the quark mass–dependent interactions, i.e., as the result of some predominance of the explicit chiral symmetry breaking terms over the dynamical chiral symmetry breaking ones for these states. Indeed, let us consider the difference

$$m_{a_0}^2 - m_\kappa^2 = 2g^2\left(\frac{1}{H_{a_0}} - \frac{1}{H_\kappa}\right) - 2(M_s + 2\hat{M})(M_s - \hat{M}). \tag{67}$$

The sign of this expression is a result of the competition of two terms. In the chiral limit both of them are zero, since at $\hat{\mu}$, $\mu_s = 0$ we obtain $\hat{M} = M_s$ and $H_{a_0} = H_\kappa$, for H_{a_0} and H_κ being positive. The splitting $H_\kappa > H_{a_0}$ is a necessary condition to get $m_{a_0} > m_\kappa$. The following terms contribute to the difference:

$$\begin{aligned} H_\kappa - H_{a_0} = {} & \kappa(h_s - \hat{h}) + 2\kappa_2(\mu_s - \hat{\mu}) \\ & - g_2(h_s^2 + \hat{h}h_s - 2\hat{h}^2) \\ & + \frac{g_3}{2}(2\mu_s h_s + \mu_s\hat{h} + \hat{\mu}h_s - 4\hat{\mu}\hat{h}) \\ & + g_5\hat{\mu}(\mu_s - \hat{\mu}) + \frac{g_6}{2}(\mu_s^2 - \hat{\mu}^2). \end{aligned} \tag{68}$$

Accordingly, from this formula we deduce the "anatomy" of the numerical fit, e.g., for set (d) (see next subsection):

$$\begin{aligned} m_{a_0}^2 - m_\kappa^2 = {} & ([0.006]_\kappa + [0.046]_{\kappa_2} + [6\times10^{-4}]_{g_2} \\ & + [0.938]_{g_3} + [0.003]_{g_5} + [-0.316]_{g_6} \\ & - [0.44]_M = 0.24)\ \mathrm{GeV}^2, \end{aligned} \tag{69}$$

where the contributions of terms with corresponding coupling [see Eq. (68)] are indicated in square brackets. The last number, marked by M, is the value of the last term from (67). It is a contribution due to the dynamical chiral symmetry breaking (in the presence of an explicit chiral symmetry breaking). One can see that the g_3 interaction is the main reason for the reverse ordering $m_{a_0} > m_\kappa$, the coupling g_6 being responsible for the fine-tuning of the result.

We now briefly comment on the role of parameters regarding the successful fit of f_π and f_K, as well as the ordering $m_K < m_\eta$. For these cases, many parameters are at work simultaneously. To illustrate this trend, we deviate (arbitrarily) the values of f_K and m_η from their empirical values, keeping the remaining observables fixed.

Let us consider first the weak decays. We take set (d) as a reference and change in the input data only $f_K = 116$ MeV. As a result we obtain that the constituent quark masses both decrease to $\hat{M} = 351$ MeV and $M_s = 533$ MeV, thus decreasing as well the normalization g in order to fulfill Eq. (62). Regarding the interaction coupling strengths, the largest deviation in absolute value is for g_2, which increases by 50%, followed by g_1 which decreases by 40%. The parameters $\{g_7, \kappa_2, g_3, g_4, g_6, \kappa\}$ decrease in the given order by $\{27, 25, 25, 22, 18, 15\}$ parts in 100, and g_8 increases by 28%. The remaining parameters have much less significant changes. We conclude that a very subtle interplay takes place involving parameters related with and without the explicit symmetry breaking in this case.

As for $m_K < m_\eta$, we take again set (d) as a reference and change in the input only the η mass, lowering it to $\eta = 490$ MeV. In this case, the largest changes are observed in $\{g_7, g_8, g_2\}$, with an increase of $\{168, 162, 93\}$ percent and a decrease in κ_2 by 73%, while a lesser increase in $\{g_4, g_6, \kappa\}$ of $\{29, 25, 20\}$ and decrease of g_3 by 16% is registered.

B. Strong decays

Let us now show the result of our global fitting of the model parameters. We study the effect of having a slightly different m_σ mass, sets (a), (b), and (d) with $m_\sigma = 550$ MeV versus set (c) with $m_\sigma = 600$ MeV, as well as having different pseudoscalar and scalar mixing angles, as described in the caption of Table I, with all other meson masses and weak decay constants remaining fixed to the values indicated there.

Table II contains the standard set of parameters, which are known from previous considerations. Their values are not much affected by the quark mass effects. We have already learned (as seen again in Table II) that higher values of g_1 lead to the lower σ mass [53]. This eight-quark interaction violates Zweig's rule, since it involves $q\bar{q}$ annihilation.

Table III contains the couplings which are responsible for the explicit chiral symmetry breaking effects in the interactions. Largest variations are observed in the couplings g_4 and g_7 in set (d) as compared to sets (a)–(c) and in g_8 between set (b) and the other sets. In the former case, it is related with the change of the scalar mixing angle and in the latter with the change in the pseudoscalar mixing angle. The coupling g_7 is seen to occur only in $(h^{(1)}_{ab})^{-1}$; thus it probes the mass spectrum of the scalars, whereas g_8 appears only in $(h^{(2)}_{ab})^{-1}$, related to the mass spectrum of the pseudoscalars. With all observables kept fixed, except the mixing angle, changes in these couplings are obviously related to them. Regarding g_4 it enters in both mass spectra. Comparing sets (a) and (c) where both θ_S and θ_P are the same, but the σ mass is different, shows that g_4 also responds to the change in the σ mass.

The calculated values of quark condensates are approximately the same for all sets: $-\langle\bar{u}u\rangle^{\frac{1}{3}} = 232$ MeV, and $-\langle\bar{s}s\rangle^{\frac{1}{3}} = 204$ MeV. Our calculated values for the constituent quark masses agree with the ones found in [8–10,47], showing their insensitivity to the new mass-dependent corrections.

In Table IV are shown the results for the strong decay widths of the scalar mesons for the four different sets. The experimental status is as follows. The mass and width of the σ meson quoted until recently had a large uncertainty, $m_\sigma = (400 \div 1200)$ MeV and a full width $\Gamma_\sigma = (600 \div 1000)$ MeV. Presently [65], it has been narrowed to $m_\sigma = (400 \div 550)$ MeV and $\Gamma_\sigma = (400 \div 700)$ MeV. The result based on the average over the dispersion analysis of [69–72] even leads to a very sharp value for the pole position $M - i\Gamma/2 = (446 \pm 6) - (276 \pm 5)$ MeV. The mass and full width of the $f_0(980)$ meson are quoted as $m_{f_0(980)} = 990 \pm 20$ MeV and $\Gamma_{f_0(980)} = 40 \div 100$ MeV and for the $a_0(980)$ meson as $m_{a_0(980)} = 980 \pm 20$ MeV and $\Gamma_{a_0(980)} = 50 \div 100$ MeV. The results for the $\kappa(800)$ quoted in the Particle Data Group (PDG) table from a Breit-Wigner fit have the pole at $(764 \pm 63^{+71}_{-54}) - i(306 \pm 149^{+143}_{-82})$ MeV.

We obtain that the σ mass and $\sigma \to \pi\pi$ decay are within the recent limits for sets (a)–(b) and (d) while set (c) has a mass larger than the upper limit by ~50 MeV. While in sets (a)–(b) and (d) the calculated width is smaller than the nominal mass of the resonance, the opposite behavior is seen in set (c). The coupling strength $\bar{g}_{\sigma\pi\pi}$ increases comparing, e.g., set (a) to (c), explaining the larger width; however, the ratio $R^\sigma = \frac{\bar{g}^\sigma_K}{\bar{g}_{\sigma\pi\pi}}$ of the σ to kaon and to the pion couplings also increases by 20%. The obtained ratio for R^σ is in agreement with the experimental value $R^\sigma_{\rm exp} = 0.5 \pm 0.1$ in [73] for sets (a)–(c) and slightly below that for set (d). We expect some effect on the width if these channels were taken into account, but only a moderate one since the coupling to pions dominates, $R^\sigma \sim 0.3 \div 0.5$.

The decay width for $\kappa(800) \to K\pi \sim 310$ MeV is smaller roughly by a factor of 2 than the quoted central value but still lies within the limits. The ratio of the couplings $\frac{\bar{g}_{\kappa K\pi}}{\bar{g}_{\sigma\pi\pi}}\frac{m^2_K}{m^2_\sigma} = 1.5$ (the ratio of meson masses corrects for the different definitions of the couplings in [73]) is

TABLE III. Explicit symmetry breaking interaction couplings. The couplings have the following units: $[\kappa_1] = \text{GeV}^{-1}$, $[\kappa_2] = \text{GeV}^{-3}$, $[g_3] = [g_4] = \text{GeV}^{-6}$, $[g_5] = [g_6] = [g_7] = [g_8] = \text{GeV}^{-4}$, $[g_9] = [g_{10}] = \text{GeV}^{-2}$. See also the caption of Table I.

Sets	κ_1	κ_2	$-g_3$	g_4	g_5	$-g_6$	$-g_7$	g_8	g_9	g_{10}
a	0*	6.14	6338	657	210	1618	105	−65	0*	0*
b	0*	5.61	6472	702	210	1668	100	−38	0*	0*
c	0*	6.12	6214	464	207	1598	133	−66	0*	0*
d	0*	6.17	6497	1235	213	1642	13.3	−64	0*	0*

TABLE IV. Strong decays of the scalar mesons; m_R is the resonance mass in MeV, $\Gamma^{\rm BW}$ and $\Gamma^{\rm Fl}$ are the Breit-Wigner width and the Flatté distribution width in MeV, $R^S = \frac{\bar{g}^S_K}{\bar{g}_\beta}$. The mixing angles are in degrees.

Set	Decays	m_R	$\Gamma^{\rm BW}$	$\Gamma^{\rm Fl}$	$\bar{g}_\beta$	$\bar{g}^S_K$	R^S	θ_P	θ_S
a	$\sigma \to \pi\pi$	550	465		1.95	0.97	0.497	−12	25
	$f_0 \to \pi\pi$	980	108	60	0.23	0.32	1.397		
	$\kappa \to K\pi$	850	310		1.2	0			
	$a_0 \to \eta\pi$	980	419	45	1.32	2.69	2.05		
b	$\sigma \to \pi\pi$	550	465		1.955	0.986	0.504	−15	25
	$f_0 \to \pi\pi$	980	108	60	0.230	0.312	1.356		
	$\kappa \to K\pi$	850	310		1.2	0			
	$a_0 \to \eta\pi$	980	459	50	1.44	2.805	1.944		
c	$\sigma \to \pi\pi$	600	635		2.39	1.52	0.61	−12	25
	$f_0 \to \pi\pi$	980	108	61	0.23	0.30	1.32		
	$\kappa \to K\pi$	850	310		1.2	0			
	$a_0 \to \eta\pi$	980	419	46	1.31	2.67	2.03		
d	$\sigma \to \pi\pi$	550	461		1.94	0.63	0.33	−12	27.5
	$f_0 \to \pi\pi$	980	62	30	0.23	0.30	3.90		
	$\kappa \to K\pi$	850	310		1.2	0			
	$a_0 \to \eta\pi$	980	420	46	1.32	2.73	2.07		

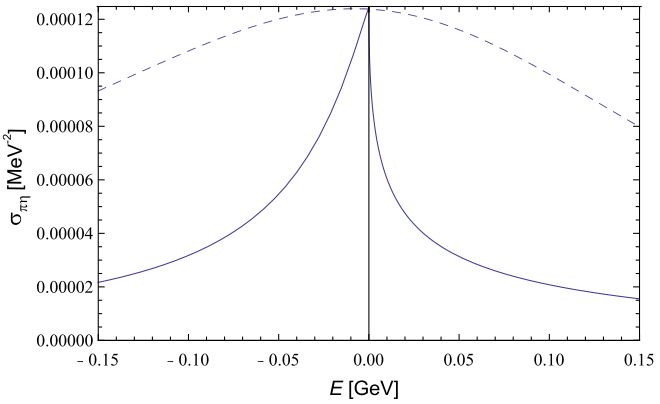

FIG. 1 (color online). The $\pi\eta$ cross section as function $E = \sqrt{s} - 2m_K$ for the a_0 resonance channel from the Flatté distribution (solid line) with parameters of set (b), $\bar{g}_{a_0\pi\eta} = 1.44$, $\bar{g}_K^{a_0} = 2.8$, $R^{a_0} = 1.944$. The width read at half peak value is $\Gamma^{\rm Fl} = 50$ MeV. The dashed line corresponds to the single $\pi\eta$ channel.

within the experimental values in [73], as opposed to the $q\bar{q}$ and $q^2\bar{q}^2$ model approaches considered in the same paper.

The widths of the $a_0(980) \to \pi\eta$ and $f_0(980) \to \pi\pi$ decays are well accommodated within a Flatté description. We read the width at half maximum of the elastic cross section in Figs. 1 and 2, respectively. Note the huge reduction in width in the case of the $a_0(980)$ meson when the kaon channels are taken into account. This possibility was already noticed by Flatté in his analysis [60]. This is explained in our description by the ratio $R^{a_0} \sim 2$ showing the dominant component to be in the coupling to the kaons.

As demonstrated in [74], the ratio $R^S = \frac{\bar{g}_K^S}{\bar{g}^\beta}$ of the couplings is a relatively stable quantity in spite of the large fluctuations in the experimental values extracted for the individual couplings. Our calculated R^S are compatible with the indicated values in [74]. It should be emphasized

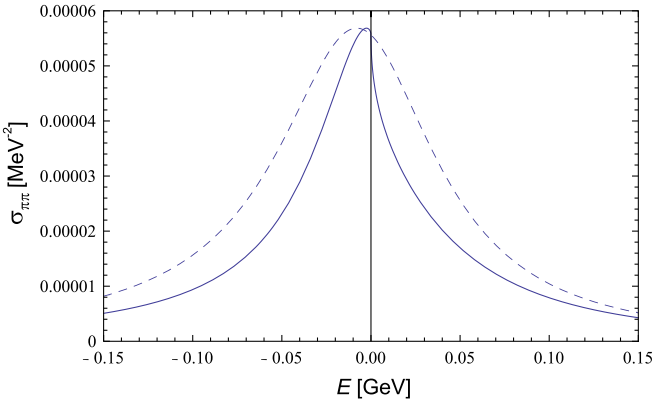

FIG. 2 (color online). The $\pi\pi$ cross section as function $E = \sqrt{s} - 2m_K$ for the f_0 resonance channel from the Flatté distribution (solid line) with parameters of set (b), $\bar{g}_{f_0\pi\pi} = 0.23$, $\bar{g}_K^{f_0} = 0.31$, $R^{f_0} = 1.36$. The width read at half peak value is $\Gamma^{\rm Fl} = 60$ MeV. The dashed line corresponds to just the two pion channel.

that the ratio $R^{f_0} = \frac{\bar{g}_K^{f_0}}{\bar{g}_{f_0\pi\pi}}$ is strongly dependent on the mixing angle θ_S of the scalar sector. As can be seen comparing sets (a)–(c) with set (d), the increase in θ_S is responsible for the larger ratio $R^{f_0} = 3.9$ in set (d), which agrees well with the experimental value $R^{f_0}_{\rm exp} = 4.21 \pm 0.46$ of BES Collaboration [75]. An often considered quantity is the crossed ratio $r = \frac{R^{f_0}}{R^{a_0}}$, usually assumed to be larger than unity. The $a_0(980)$ does not depend on the θ_S mixing angle [an eventual correlation with the $f_0(980)$ meson through isospin mixing is discarded here] but does depend on the pseudoscalar θ_P angle through its decay into the $\pi\eta$. The θ_P is fixed in the pseudoscalar sector to yield the correct η and η' masses, as well as their radiative two photon decay widths. Therefore the ratio R^{a_0} of the a_0 couplings to kaons and to the $\pi\eta$ channels remains approximately constant for all parameter sets $(R^{a_0})^{-1} \sim 0.5$. This value is not too bad in comparison with the experimental quoted ratio $(R^{a_0}_{\rm exp})^{-1} = 0.75 \pm 0.11$ [76]. Requiring the ratio $r > 1$ further constrains the angle to be larger than $\theta_S \sim 26°$.

On the other hand, the ratio R^{f_0} increases until θ_S reaches ideal mixing. In the interval $\theta_{id} < \theta_S \leq \frac{\pi}{4}$, it decreases but stays much larger than the experimental accepted ratio; e.g., at $\theta_S = 44°$, one has $R^{f_0} \sim 11$. The combined requirements $r > 1$ and $R^{f_0}_{\rm exp}$ confine the mixing angle to the narrow window $27° < \theta_S < 28°$. From the point of view of the calculated strong decay widths, however, the somewhat smaller angle $\theta_S = 25°$ is also acceptable. Our interval of values for the mixing angle $25° < \theta_S < 28°$, corresponding to $-10.3° < \bar{\psi} < -7.3°$, are within the values $-14° < \bar{\psi} < -3°$ estimated in [77], more specifically $\bar{\psi} \sim -9°$ if a Flatté distribution is used in a complementarity approach of chiral perturbation theory and the linear sigma model.

C. Radiative decays

The two photon decays of the pseudoscalars are in very good agreement with data (Table VI); the π^0 and η in two photons are within the experimental error bars; and the η' decay lies 10% above the upper limit for sets (a), (c) and (d), i.e., $\theta_P = -12°$. In the case of set (b), $\theta_P = -15°$, the result for the η' decay is at the upper margin, and for η about 10% above the upper boundary.

For the radiative widths of σ (see Table V), there is a large spread in the experimental data from different facilities. Our results for $\sigma \to \gamma\gamma$ only account for about 20% of the value (1.2 ± 0.4) KeV [78] obtained from the nucleon electromagnetic polarizabilities, which is one of the lowest estimates for this width. For the $f_0(980) \to \gamma\gamma$, the PDG average is quoted as $(0.29^{+0.07}_{-0.06})$ KeV. Sets (a)–(c) yield approximately 20% and set (e) 30% of this value. These results meet the current expectations that a direct coupling to the photons via a quark loop are not sufficient to account for the observed radiative widths of these mesons.

TABLE V. Radiative decays of the scalar mesons $\Gamma_{S\gamma\gamma}$ in KeV; m_R is the resonance mass in MeV.

Set a	m_R	$\Gamma_{S\gamma\gamma}$	Set b	m_R	$\Gamma_{S\gamma\gamma}$	Set c	m_R	$\Gamma_{S\gamma\gamma}$	Set d	m_R	$\Gamma_{S\gamma\gamma}$
$\sigma \to \gamma\gamma$	550	0.212	$\sigma \to \gamma\gamma$	550	0.212	$\sigma \to \gamma\gamma$	600	0.277	$\sigma \to \gamma\gamma$	550	0.210
$f_0 \to \gamma\gamma$	980	0.055	$f_0 \to \gamma\gamma$	980	0.055	$f_0 \to \gamma\gamma$	980	0.055	$f_0 \to \gamma\gamma$	980	0.080
$a_0 \to \gamma\gamma$	980	0.389	$a_0 \to \gamma\gamma$	980	0.386	$a_0 \to \gamma\gamma$	980	0.392	$a_0 \to \gamma\gamma$	980	0.383

A natural question arises then why in our approach the strong widths can be described reasonably well in all channels and the radiative ones fall short of the empirical values for the σ, f_0 decays. This can be understood: only the strong decays probe directly the multiquark couplings g_i contained in the stationary phase (SPA) piece (28) of the total interaction Lagrangian (49). Since this part of the Lagrangian has no derivative terms, only the heat kernel (HK) Lagrangian involves the electromagnetic interaction, after minimal coupling. The information of the SPA conditions which leaks through the gap equations to the electromagnetic sector is rather weak; it is contained only in the wave function normalization which is the same for all mesons, and the quark constituent masses and scale Λ which remain approximately constant in all parameter sets. Thus, effectively, the two photon decays of the scalars yield a clean signature whether the electromagnetic decay of the mesons proceeds dominantly through a $q\bar{q}$ channel or not.

This in turn ties up with the strength distribution in the HK and SPA contributions to the coupling g_{SPP} shown in Tables VII and VIII for set (d). The HK piece relates directly to the meson-$q\bar{q}$ channel, the SPA part to the higher order multiquark interactions.

Consider first the a_0 meson: the calculated $a_0(980) \to \gamma\gamma \sim 0.39$ KeV overestimates the present average PDG value $0.21^{+0.08}_{-0.04}$ and points within our approach to the dominance of the direct one quark loop coupling to photons of this meson.

This is corroborated by the fact that the large bare width that we obtain for the $a_0 \to \pi\eta$ decay is shown to stem mainly from the HK coefficient represented with 80% of the total strength; see Table VII. The a_0 meson in the $q\bar{q}$ picture is composed only of u and d quarks; thus, its coupling to the $K\bar{K}$ mesons requires a flavor change at the kaon vertices, as opposed to the $\eta\pi$ case. As can be seen from a similar decomposition in HK and SPA contributions of the $a_0 K\bar{K}$ coupling in Table VIII, it is much more favorable to couple to the kaons through the multiquark vertices, which now represent 80% of the total strength instead. Therefore for the overall strong decay width, it is important to take this mode into account through the two-channel Flatté distribution. From the point of view of the two photon decay of a_0, we note that a $\pi\eta$ loop does not couple directly to two photons [79] and the decay proceeds through the quark loop of u or d quarks with the large strength of the corresponding HK component. To access the dominant SPA component the two photon decay would have to proceed through coupling to the $K\bar{K}$ loop, a subleading process in N_c counting as compared to the direct $q\bar{q}$ loop. Furthermore, due to the relatively large mass of the kaons, this loop is not expected to contribute significantly.

Now let us analyze the σ, f_0 channels: there are substantial contributions or cancellations from the SPA part. For the $f_0\pi\pi$ and $f_0 K\bar{K}$ cases, one sees that the strength in the SPA coefficient is in magnitude about $\frac{2}{3}$ of the HK coefficient for both cases, but changes relative sign in the latter. In the $\sigma\pi\pi$ and $\sigma K\bar{K}$ cases, the cancellations occur in both cases, with the SPA piece contributing about half of the HK part. There is a subtle interplay about the HK and SPA coefficients which finally add up to the correct description of the mass spectra and strong decays of these mesons. The lack of a pronounced dominance of the HK has as a consequence that the $q\bar{q}$ coupling of these mesons to the photons represents only a fraction of the total width. The remaining strength must derive from the multiquark channels which should be included in an extra step, taking into account explicitly meson loop contributions.

Regarding the strong decay of the f_0, one can further infer that because of the stronger participation of the multiquark interactions and because of cancellations in the kaon

TABLE VI. Anomalous decays $\Gamma_{P\gamma\gamma}$ for sets (a) and (c) in KeV, corresponding to $\theta_P = -12°$; m_R is the particle mass in MeV. [For set (b), corresponding to $\theta_P = -15°$, we have $\Gamma_{\eta\gamma\gamma} = 0.6$ KeV, $\Gamma_{\eta'\gamma\gamma} = 4.8$ KeV.]

Decays	m_R	$\Gamma_{P\gamma\gamma}$	$\Gamma^{\rm exp}_{P\gamma\gamma}$ [65]
$\pi^0 \to \gamma\gamma$	136	0.00798	$0.00774637 \div 0.00810933$
$\eta \to \gamma\gamma$	547	0.5239	$(39.31 \pm 0.2)\%\Gamma_{\rm tot} = 0.508 \div 0.569$
$\eta' \to \gamma\gamma$	958	5.225	$(2.18 \pm 0.08)\%\Gamma_{\rm tot} = 3.99 \div 4.70$

TABLE VII. The coefficients coef$^{\rm HK}$ and coef$^{\rm SPA}$ of the heat kernel and of the SPA contributions to the total value of the coupling $g_{SP_1P_2}$ resulting from the interaction Lagrangian for the open decay channels. Values are for the neutral channels. Units are in GeV.

$g_{SP_1P_2}$	coef$^{\rm HK}/g^3$	coef$^{\rm SPA}/g^3$	Total$/g^3$
$\sigma\pi^0\pi^0$	-0.0450	0.0215	-0.0235
$f_0\pi^0\pi^0$	-0.0061	-0.0047	-0.0109
$\kappa^0\bar{K}^0\pi^0$	0.0660	-0.0257	0.0403
$a_0^0\eta\pi^0$	-0.0666	-0.0178	-0.0844

TABLE VIII. The coefficients coef^{HK} and coef^{SPA} of the heat kernel and of the SPA contributions to the total value of the coupling $g_{SK\bar{K}}$ resulting from the interaction Lagrangian. Values are for the neutral channels. Units are in GeV.

$g_{SK\bar{K}P_2}$	$\text{coef}^{\text{HK}}/g^3$	$\text{coef}^{\text{SPA}}/g^3$	Total/g^3
$\sigma K\bar{K}$	−0.041	0.0178	−0.0232
$f_0 K\bar{K}$	0.118	−0.081	0.0372
$a_0^0 K\bar{K}$	0.0246	0.0968	0.121

channel as opposed to the pion channel, a coupling to the kaon channel through the Flatté approach is not imperative to obtain a reasonable magnitude of the width, as seen from Table IV.

Rescattering effects have been shown in several approaches to yield the main contribution, e.g., for the $\sigma \to \gamma\gamma$ extracted from the dispersion analysis of $\gamma\gamma \to \pi^0\pi^0$ [81]. Claims for a tetraquark structure [29] of the σ meson were forwarded, e.g., in [82], and in [83] interpreted as pion and kaon loop contributions. Our approach sheds light on these phenomena from a different angle.

Finally we mention that the radiative decays of the scalar mesons have been calculated a long time ago in a variant of the NJL model, with and without meson loop contributions [84]. The amplitudes differ from ours in two key aspects: we use the unified description for all nonanomalous decays based on the generalized heat kernel approach which leads (i) to a common wave function normalization for all mesons that implies the reduction factor of $\sim\frac{2}{3}$ in the amplitude and in the case of the radiative decays to (ii) the regularized one loop integrals carrying the factors $(\frac{\Lambda^2}{\Lambda^2+M_i^2})^2$, in spite of the integrals being finite. The latter reduces the amplitude by approximately half. The combined effect is a dramatic reduction by a factor ∼10 in the decay widths, as compared to [84] for the quark loop contribution. Thus, caution must be used when it comes to interpreting and comparing our numerical results with seemingly related model calculations, e.g., [85,86].

Summarizing the results of Secs. IV B and IV C, the strong decays calculated from our tree level meson couplings encode leading and higher order N_c and multiquark effects in combinations that account for the main bulk of the empirical widths. The two photon decays of the scalars at leading order of the bosonized Lagrangian yield complementary information, testing whether the direct one quark loop coupling to photons is the dominant decay process. We obtained that the a_0 meson decay into two photons proceeds mainly through the $q\bar{q}$ loop, whereas for the σ, f_0 mesons we conclude that higher order multiquark interactions are necessary to account for the observed widths. This does not mean that the a_0 meson is mainly a $q\bar{q}$ state, but that the multiquark component with the large strength in the two kaon channel, important for the reduction of the $a_0\pi\eta$ strong decay width, is not the leading process in the two photon decay of this meson.

V. CONCLUDING REMARKS

In this paper, we have generalized the effective multiquark Lagrangians of the NJL type by including higher order terms in the current quark-mass expansion. The procedure is based on the very general assumption that the scale of spontaneous chiral symmetry breaking determines the hierarchy of local multiquark interactions. As a consequence, one can distinguish a finite subset of vertices which are responsible for the explicit chiral symmetry breaking at each order considered. We have classified these vertices at next-to-leading order and studied the phenomenological consequences of their inclusion in the Lagrangian.

We are led to a subset of ten quark mass–dependent interactions which enter the Lagrangian at the same order as the 't Hooft determinant and eight quark terms previously analyzed in the literature. From these, three are related with the Manohar-Kaplan ambiguity, and the remaining seven with genuinely new vertices. These new terms carry either signatures of violation of Zweig's rule or of admixtures of $q^2\bar{q}^2$ states to the quark-antiquark ones and are thus potentially interesting candidates in the quest to analyze the structure and interaction dynamics of the low lying mesons.

We have derived the bosonized Lagrangian up to cubic order in the meson fields, from which we obtain the meson spectra and their two-body strong, weak, and electromagmetic decays. Here are our main conclusions.

(1) We fit the low lying pseudoscalar spectrum (the pseudo-Goldstone 0^{-+} nonet) and weak decay constants of the pion and the kaon to perfect accuracy. The fitting of the η-η' mass splitting together with the overall successful description of the whole set of low-energy pseudoscalar characteristics is actually a solution for a long-standing problem of NJL-type models. We have found that the quark mass–dependent interaction terms mainly responsible for the fit belong to the class of Okubo-Zweig-Iizuka (OZI)-violating interactions. They represent additional corrections to the 't Hooft $U_A(1)$ breaking mechanism. In the interaction terms independent of the quark masses, we observe, however, that the g_2 coupling of the non-OZI-violating $8q$ interactions carrying the signature of the $q^2\bar{q}^2$ states are also relevant in fitting the f_π, f_K values as well as for the ordering $m_K < m_\eta$.

(2) We are also capable of describing the spectrum of the light scalar nonet. In this case, we identify the quark-mass interaction terms related with the four quark admixtures to be the main source of the fit associated with the $a_0(980)$ and $\kappa(800)$ meson masses. The primary term responsible for the correct ordering carries interaction strength g_3, and some fine-tuning is due to the g_6 term.

(3) Regarding the mixing angle of the singlet-octet scalar states θ_S, we have found that its value is

particularly sensitive to the interaction terms proportional to g_4 and g_7, which are OZI-violating. Together with the result that the strength g_1 of the eight quark OZI-violating and quark mass–independent interaction terms studied in earlier papers dictates the mass of the $\sigma(500)$ meson, we conclude that these states are strongly affected by OZI-violating short range forces.

(4) The calculation of the strong decays of the scalar mesons has revealed that the present Lagrangian is capable of accounting for the decay widths within the actual margins of empirical data. We corroborate other model calculations in which the coupling of the $f_0(980)$ and $a_0(980)$ mesons to the $K\bar{K}$ channel is needed for the description of the decays $f_0(980) \to \pi\pi$ and $a_0(980) \to \pi\eta$. We find that this coupling is most crucial for the latter process.

(5) The radiative decays of the scalar mesons into two photons show that the main channel for the $a_0(980)$ decay proceeds through coupling to a quark-antiquark state, while the radiative decays of singlet-octet states σ, f_0 must proceed through more complex structures. We refer to the full discussion given in Secs. IV B and IV C.

(6) Finally, the radiative decays of the pseudoscalars are in very good agreement with data.

ACKNOWLEDGMENTS

This work has been supported by the Fundação para a Ciência e Tecnologia project: CERN/FP/116334/2010, developed under the initiative QREN, financed by UE/FEDER through COMPETE—Programa Operacional Factores de Competitividade. This research is part of the EU Research Infrastructure Integrating Activity Study of Strongly Interacting Matter (HadronPhysics3) under the 7th Framework Programme of EU, Grant No. 283286.

[1] Y. Nambu and G. Jona-Lasinio, Phys. Rev. **122**, 345 (1961); **124**, 246 (1961).
[2] V. G. Vaks and A. I. Larkin, Zh. Éksp. Teor. Fiz. **40**, 282 (1961) [Sov. Phys. JETP **13**, 192 (1961)].
[3] G. 't Hooft, Phys. Rev. D **14**, 3432 (1976).
[4] G. 't Hooft, Phys. Rev. D **18**, 2199 (1978).
[5] V. Bernard, R. L. Jaffe, and U.-G. Meißner, Phys. Lett. B **198**, 92 (1987).
[6] V. Bernard, R. L. Jaffe, and U.-G. Meißner, Nucl. Phys. **B308**, 753 (1988).
[7] H. Reinhardt and R. Alkofer, Phys. Lett. B **207**, 482 (1988).
[8] S. Klimt, M. Lutz, U. Vogl, and W. Weise, Nucl. Phys. **A516**, 429 (1990).
[9] U. Vogl, M. Lutz, S. Klimt, and W. Weise, Nucl. Phys. **A516**, 469 (1990).
[10] U. Vogl and W. Weise, Prog. Part. Nucl. Phys. **27**, 195 (1991).
[11] M. Takizawa, K. Tsushima, Y. Kohyama, and K. Kubodera, Nucl. Phys. **A507**, 611 (1990).
[12] S. P. Klevansky, Rev. Mod. Phys. **64**, 649 (1992).
[13] T. Hatsuda and T. Kunihiro, Phys. Rep. **247**, 221 (1994).
[14] V. Bernard, A. H. Blin, B. Hiller, U.-G. Meißner, and M. C. Ruivo, Phys. Lett. B **305**, 163 (1993).
[15] V. Dmitrasinovic, Nucl. Phys. **A686**, 379 (2001).
[16] M. C. Birse, T. D. Cohen, and J. A. McGovern, Phys. Lett. B **388**, 137 (1996).
[17] K. Naito, M. Oka, M. Takizawa, and T. Umekawa, Prog. Theor. Phys. **109**, 969 (2003).
[18] A. A. Osipov, B. Hiller, and J. da Providência, Phys. Lett. B **634**, 48 (2006).
[19] A. A. Andrianov and V. A. Andrianov, Theor. Math. Phys. **94**, 3 (1993).
[20] A. A. Andrianov and V. A. Andrianov, Int. J. Mod. Phys. A **08**, 1981 (1993).
[21] D. Ebert and H. Reinhardt, Nucl. Phys. **B271**, 188 (1986).
[22] J. Bijnens, C. Bruno, and E. de Rafael, Nucl. Phys. **B390**, 501 (1993).
[23] Z. Zhang and T. Kunihiro, arXiv:1005.1882.
[24] J. Gasser and H. Leutwyler, Phys. Rep. **87**, 77 (1982).
[25] S. Weinberg, Physica (Amsterdam) **96**, 327 (1979).
[26] H. Pagels, Phys. Rep. **16**, 219 (1975).
[27] J. Gasser and H. Leutwyler, Ann. Phys. (N.Y.) **158**, 142 (1984).
[28] J. Gasser and H. Leutwyler, Nucl. Phys. **B250**, 465 (1985).
[29] R. J. Jaffe, Phys. Rev. D **15**, 267 (1977); **15**, 281 (1977).
[30] D. Black, A. H. Fariborz, E. Sannino, and J. Schechter, Phys. Rev. D **59**, 074026 (1999).
[31] D. Wong and K. F. Liu, Phys. Rev. D **21**, 2039 (1980).
[32] S. Narrison, Phys. Lett. B **175**, 88 (1986).
[33] E. van Beveren, T. A. Rijken, K. Metzger, C. Dullemond, G. Rupp, and J. E. Ribeiro, Z. Phys. C **30**, 615 (1986).
[34] J. I. Latorre and P. Pascoal, J. Phys. G **11**, L231 (1985).
[35] M. Alford and R. L. Jaffe, Nucl. Phys. **B509**, 312 (1998).
[36] N. N. Achasov, S. A. Devyanin, and D. N. Shestakov, Z. Phys. C **16**, 55 (1982).
[37] N. Isgur and J. Weinstein, Phys. Rev. D **41**, 151 (1990).
[38] A. H. Fariborz, R. Jora, and J. Schechter, Phys. Rev. D **77**, 094004 (2008).
[39] A. H. Fariborz, R. Jora, and J. Schechter, Phys. Rev. D **79**, 074014 (2009).
[40] F. E. Close and N. A. Törnqvist, J. Phys. G **28**, R249 (2002).
[41] E. Klempt and A. Zaitsev, Phys. Rep. **454**, 1 (2007).
[42] A. A. Osipov, B. Hiller, A. H. Blin, and J. da Providência, Phys. Lett. B **650**, 262 (2007).

[43] R. Gatto and M. Ruggieri, Phys. Rev. D **82**, 054027 (2010).
[44] R. Gatto and M. Ruggieri, Phys. Rev. D **83**, 034016 (2011).
[45] M. Frasca and M. Ruggieri, Phys. Rev. D **83**, 094024 (2011).
[46] R. Gatto and M. Ruggieri, Lect. Notes Phys. **871**, 87 (2013).
[47] A. Manohar and H. Georgi, Nucl. Phys. **B234**, 189 (1984).
[48] A. A. Osipov, B. Hiller, and A. H. Blin, Eur. Phys. J. A **49**, 14 (2013).
[49] D. B. Kaplan and A. V. Manohar, Phys. Rev. Lett. **56**, 2004 (1986).
[50] H. Leutwyler, Nucl. Phys. **B337**, 108 (1990).
[51] J. F. Donoghue and D. Wyler, Phys. Rev. D **45**, 892 (1992).
[52] H. Leutwyler, Phys. Lett. B **374**, 163 (1996).
[53] A. A. Osipov, B. Hiller, A. H. Blin, and J. da Providência, Ann. Phys. (Amsterdam) **322**, 2021 (2007).
[54] A. A. Osipov and B. Hiller, Phys. Lett. B **515**, 458 (2001).
[55] A. A. Osipov and B. Hiller, Phys. Rev. D **63**, 094009 (2001).
[56] A. A. Osipov and B. Hiller, Phys. Rev. D **64**, 087701 (2001).
[57] M. K. Volkov and A. A. Osipov, Yad. Fiz. **41**, 785 (1985) [Sov. J. Nucl. Phys. **41**, 500 (1985)].
[58] A. A. Osipov, H. Hansen, and B. Hiller, Nucl. Phys. **A745**, 81 (2004).
[59] P. Kroll, Int. J. Mod. Phys. A **20**, 331 (2005).
[60] S. M. Flatté, Phys. Lett. **63B**, 224 (1976); **63**, 228 (1976).
[61] S. Adler, Phys. Rev. **177**, 2426 (1969).
[62] J. S. Bell and R. Jackiw, Nuovo Cimento A **60**, 47 (1969).
[63] S. L. Adler and W. A. Bardeen, Phys. Rev. **182**, 1517 (1969).
[64] B. Bajc, A. H. Blin, B. Hiller, M. C. Nemes, A. A. Osipov, and M. Rosina, Nucl. Phys. **A604**, 406 (1996).
[65] J. Beringer *et al.* (Particle Data Group), Phys. Rev. D **86**, 010001 (2012).
[66] M. K. Volkov, Ann. Phys. (N.Y.) **157**, 282 (1984).
[67] M. K. Volkov, Fiz. Elem. Chastits At. Yadra **17**, 433 (1986) [Sov. J. Part. Nucl. **17**, 186 (1986)].
[68] M. X. Su, L. Y. Xiao, and H. Q. Zheng, Nucl. Phys. **A792**, 288 (2007).
[69] G. Colangelo, J. Gasser, and H. Leutwyler, Nucl. Phys. **B603**, 125 (2001).
[70] I. Caprini, G. Colangelo, and H. Leutwyler, Phys. Rev. Lett. **96**, 132001 (2006).
[71] R. Garcia-Martin, R. Kaminski, J. R. Pelaez, and J. Ruiz de Elvira, Phys. Rev. Lett. **107**, 072001 (2011).
[72] B. Moussalam, Eur. Phys. J. C **71**, 1814 (2011).
[73] D. V. Bugg, Eur. Phys. J. C **47**, 57 (2006); **47**, 45 (2006).
[74] V. Baru, J. Haidenbauer, C. Hanhart, A. Kudryavtsev, and U.-G. Meißner, Eur. Phys. J. A **23**, 523 (2005).
[75] M. Ablikim *et al.*, Phys. Lett. B **607**, 243 (2005).
[76] B. Hyams *et al.*, Nucl. Phys. **B64**, 134 (1973).
[77] A. Bramon, R. Escribano, J. L. Lucio M., M. Napsuciale, and G. Pancheri, Eur. Phys. J. C **26**, 253 (2002).
[78] J. Bernabeu and J. Prades, Phys. Rev. Lett. **100**, 241804 (2008).
[79] In absence of the vector mesons. Their inclusion leads to this possibility through additional vertices $VP\gamma$, where V and P stand for vector and pseudosaclar mesons, respectively [80].
[80] N. N. Achasov and G. N. Shestakov, Phys. Rev. D **81**, 094029 (2010).
[81] J. A. Oller, L. Roca, and C. Schat, Phys. Lett. B **659**, 201 (2008).
[82] F. Giacosa, Phys. Rev. D **74**, 014028 (2006).
[83] N. N. Achasov and G. N. Shestakov, Phys. Rev. D **77**, 074020 (2008).
[84] D. Ebert, T. Feldmann, and M. K. Volkov, Int. J. Mod. Phys. A **12**, 4399 (1997).
[85] M. K. Volkov, E. A. Kuraev, and Yu. M. Bystritsky, arXiv:0904.2484.
[86] M. Schumacher, J. Phys. G **38**, 083001 (2011).